PAUL STEVENSON || UNIVERSITY OF SURREY

USING MEAN-FIELD DYNAMICS TO UNDERSTAND DENSITY FUNCTIONALS

+ A. S. Umar, J. A. Maruhn, P.-G. Reinhard, P. M. Goddard, E. B. Suckling, S. Fracasso

OVERVIEW

- Skyrme EDF
- tensor terms in collisions
- continuum BCs
- fission
- nuclear matter & giant resonances

TIME-DEPENDENT HARTREE-FOCK

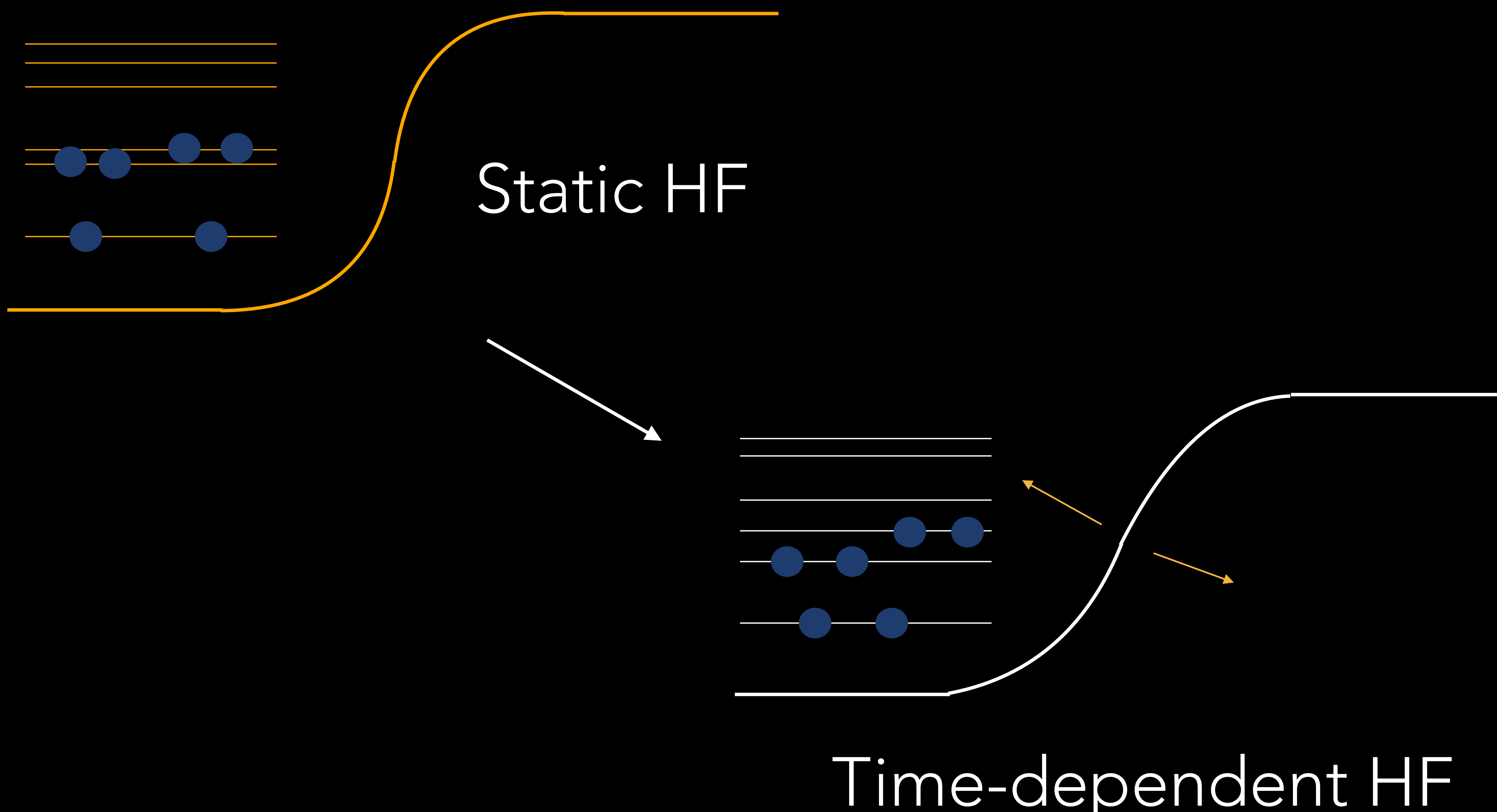

SKYRME DENSITY FUNCTIONAL

- T. H. R. Skyrme, Nucl. Phys. 9, 615 (1959)

It is generally believed that the most important part of the two-body interaction can be represented by a contact potential, i.e. by constant $t(\mathbf{k}', \mathbf{k})$; this suggests an expansion in powers of $\mathbf{k}'$ and $\mathbf{k}$. If this expansion is stopped at the quadratic terms only a small number of undetermined coefficients occur, and an attempt can be made to determine these by

$$t_{12} = \delta(\mathbf{r}_1 - \mathbf{r}_2) t(\mathbf{k}', \mathbf{k})$$

$$\begin{aligned} t(\mathbf{k}', \mathbf{k}) = {} & t_0(1 + x_0 P^\sigma) + \tfrac{1}{2} t_1 (1 + x_1 P^\sigma)(\mathbf{k}'^2 + \mathbf{k}^2) \\ & + t_2[1 + x_2(P^\sigma - \tfrac{4}{5})]\mathbf{k}' \cdot \mathbf{k} \\ & + \tfrac{1}{2} T[\boldsymbol{\sigma}_1 \cdot \mathbf{k} \boldsymbol{\sigma}_2 \cdot \mathbf{k} - \tfrac{1}{3} \boldsymbol{\sigma}_1 \cdot \boldsymbol{\sigma}_2 \mathbf{k}^2 + \text{conj.}] \\ & + \tfrac{1}{2} U[\boldsymbol{\sigma}_1 \cdot \mathbf{k}' \boldsymbol{\sigma}_2 \cdot \mathbf{k} - \tfrac{1}{3} \boldsymbol{\sigma}_1 \cdot \boldsymbol{\sigma}_2 \mathbf{k}' \cdot \mathbf{k} + \text{conj.}] \\ & + V[i(\boldsymbol{\sigma}_1 + \boldsymbol{\sigma}_2) \cdot \mathbf{k}' \times \mathbf{k}], \end{aligned}$$

$$t_{123} = \delta(\mathbf{r}_1 - \mathbf{r}_2)\delta(\mathbf{r}_3 - \mathbf{r}_1) t_3$$

SKYRME ENERGY DENSITY FUNCTIONAL

$$E=\int d^3r \sum_{t=0,1}\Big(C_t^{\rho}[\rho_0]\rho_t^2 + C_t^{s}[\rho_0]s_t^2 + C_t^{\Delta\rho}\rho_t\nabla^2\rho_t + C_t^{\nabla\cdot s}(\nabla\cdot s_t)^2 +$$

$$C_t^{\Delta s}s_t\nabla^2 s_t + C_t^{\tau}(\rho_t\tau_t - j^2) + C_t^{T}(s_t\cdot T_t - J_{t,\mu\nu}J_{t,\mu\nu}) +$$

$$C_t^{F}(s_t\cdot F_t - \tfrac{1}{2}J_{t,\mu\mu} - \tfrac{1}{2}J_{t,\mu\nu}J_{t,\nu\mu}) + C_t(\rho_t\nabla\cdot J_t + s_t\cdot\nabla\times j_t)$$

adjustable coefficients: $C_t^{\rho}[\rho_0]$, $C_t^{s}[\rho_0]$, $C_t^{\Delta\rho}$, $C_t^{\nabla\cdot s}$, $C_t^{\Delta s}$, C_t^{τ}, C_t^{T}, C_t^{F} & C_t

time-even densities & currents:

$\rho_q(r)=\rho_q(r,r')|_{r=r'}$

$\tau_q(r)=\nabla\cdot\nabla'\rho_q(r,r')|_{r=r'}$

$J_{q,\mu\nu}(r)=-\tfrac{1}{2}\, i\, (\nabla_\mu-\nabla'_\mu)s_{q,\nu}(r,r')|_{r=r'}$

time-odd densities & currents:

$s_q(r)=s_q(r,r')|_{r=r'}$

$j_q(r) =-\tfrac{1}{2}\, i\, (\nabla-\nabla')\rho_q(r,r')|_{r=r'}$

$T_q(r)=\nabla\cdot\nabla' s_q(r,r')|_{r=r'}$

$F_q(r)=\tfrac{1}{2}\sum_\nu(\nabla_\mu\nabla'_\nu+\nabla'_\mu\nabla_\nu)s_{q,\nu}(r,r')|_{r=r'}$

UPPER FUSION THRESHOLD IN $^{16}O+^{16}O$

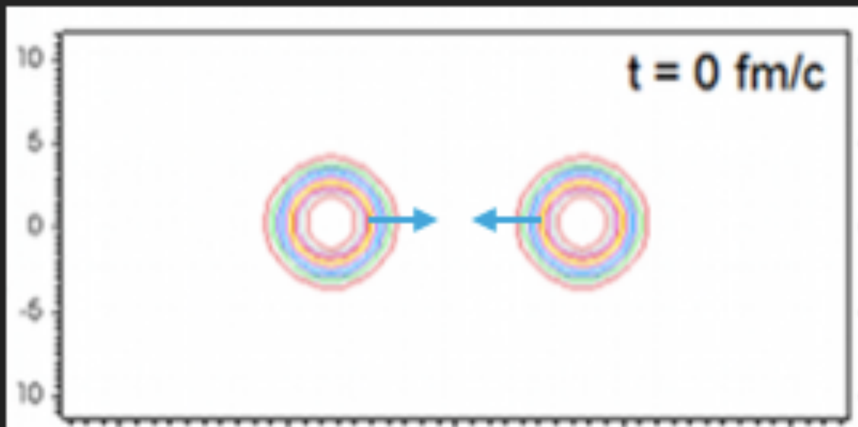

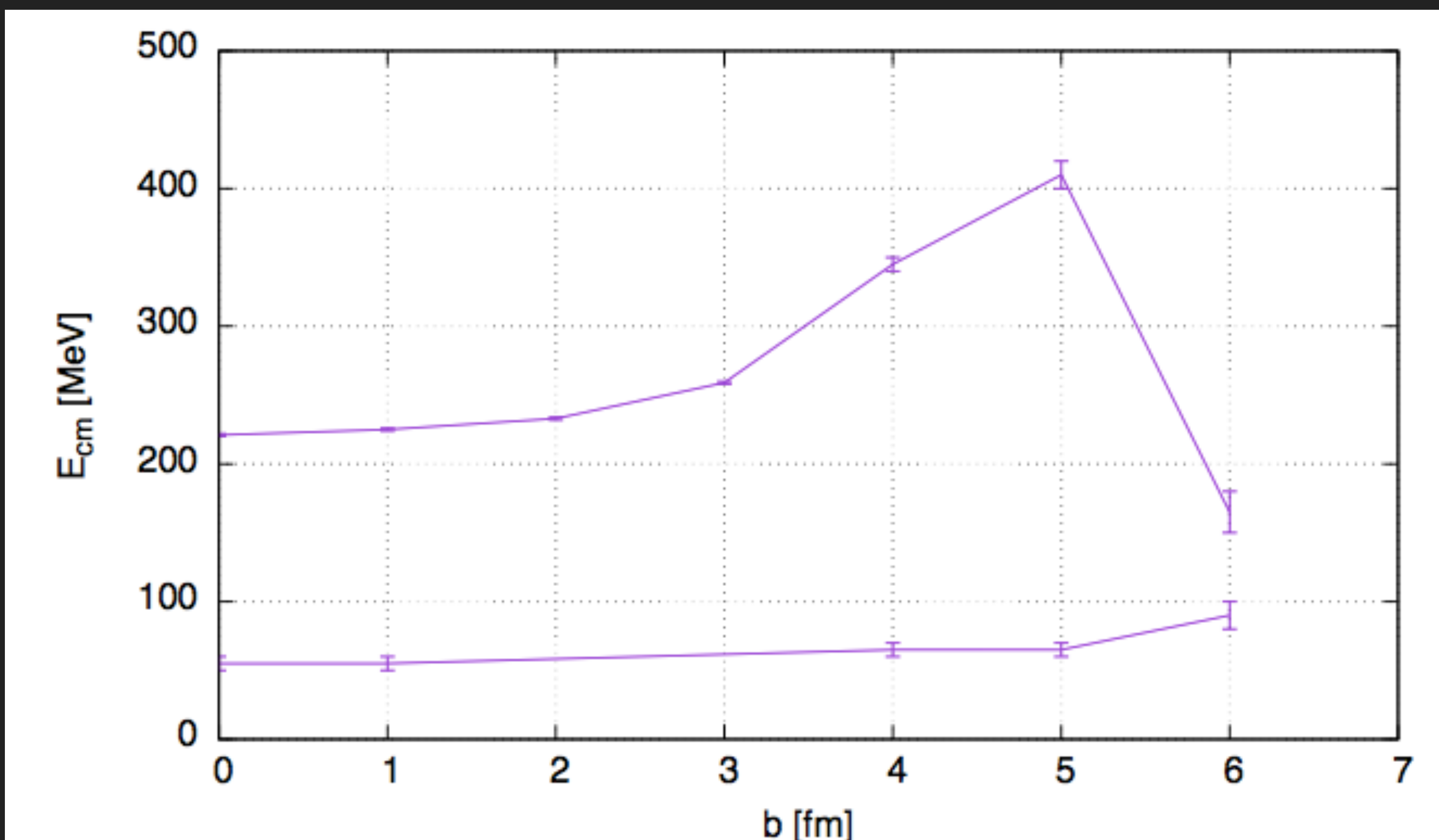

Can map out fusion landscape as a function of b and E_{CM}.

Lower boundary is due to Coulomb interaction and is insensitive to the force, but the upper boundary is force-dependent

(N.B this sample landscape shows $^{40}Ca+^{40}Ca$

UPPER FUSION THRESHOLDS IN $^{16}O+^{16}O$

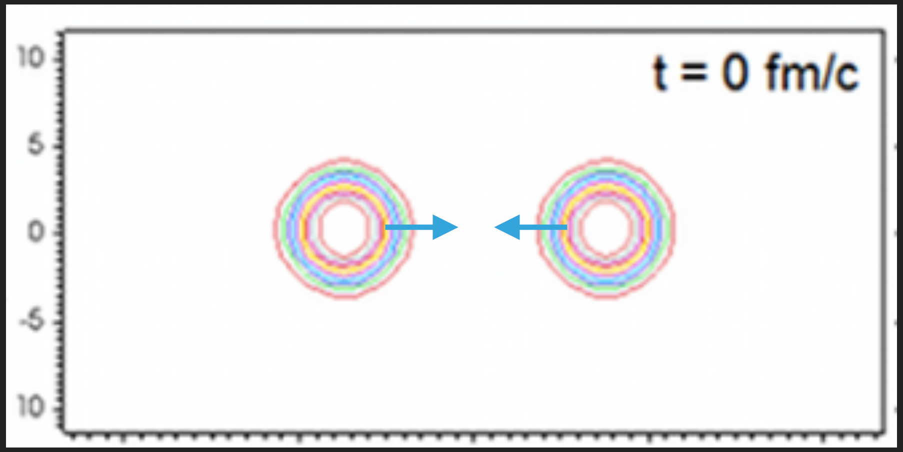

Force	Threshold (MeV)
SkM* (basic)	77
SkM* (inc. J^2)	71
SkM* (full)	73
SLy5 (full)	68
SLy5t	65
$T12$	61
$T14$	69
$T22$	64
$T24$	71
$T26$	82
$T42$	69
$T44$	79
$T46$	87

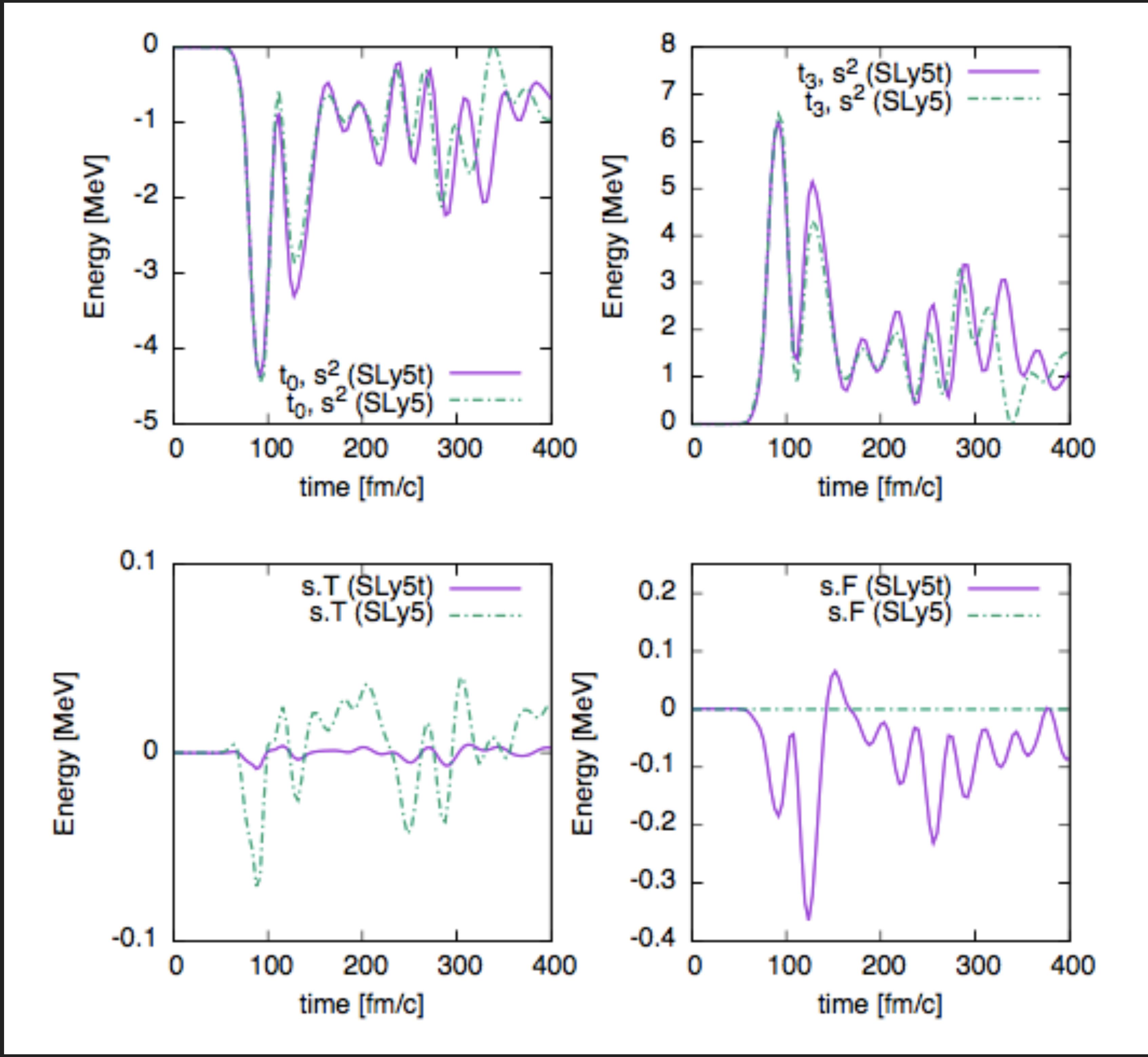

ROLE OF J^2 TENSOR

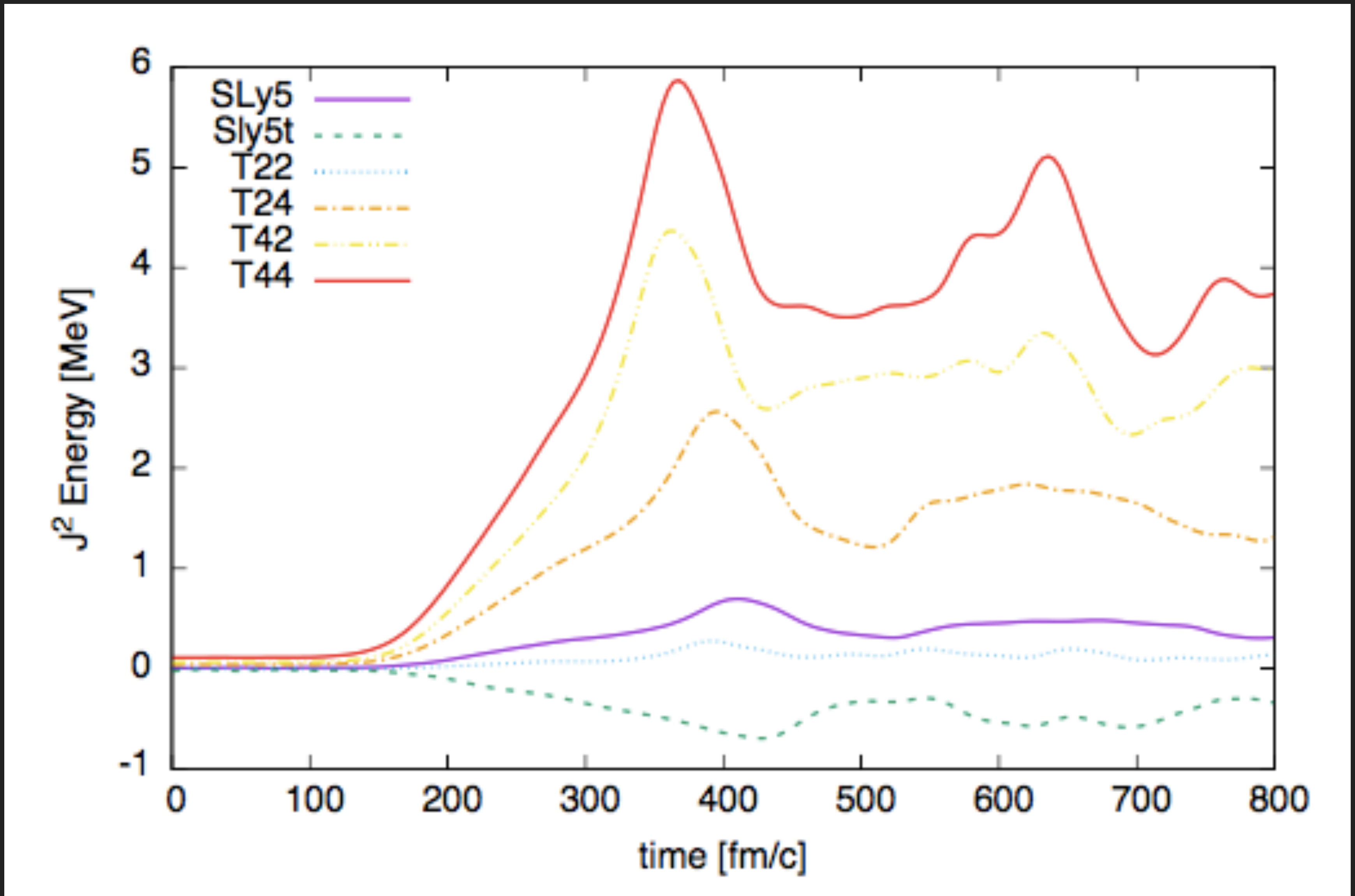

T22 (TOP) VS T24 (BOTTOM) $^{16}O+^{16}O$ @ 68 MEV

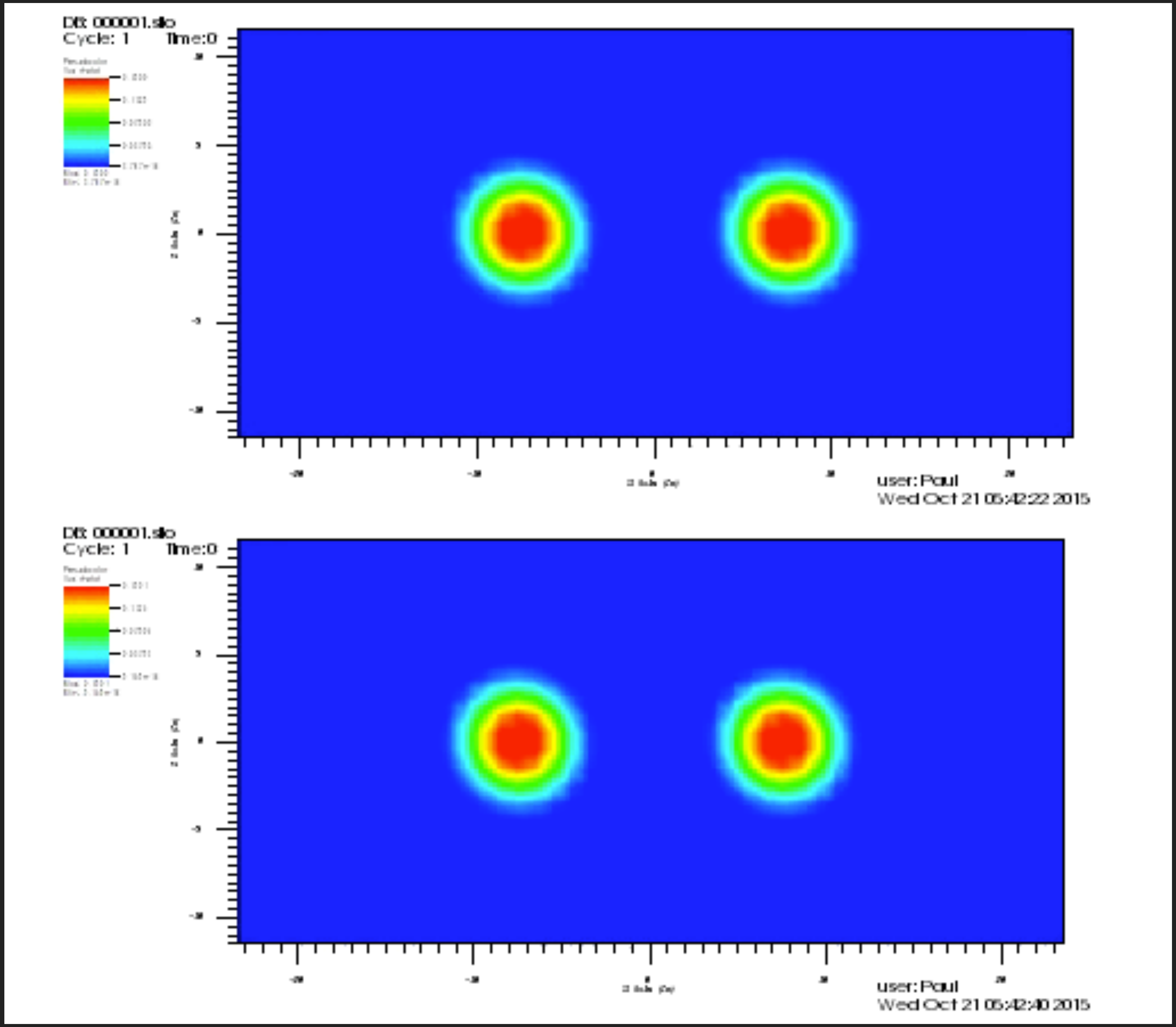

SEE ALSO…

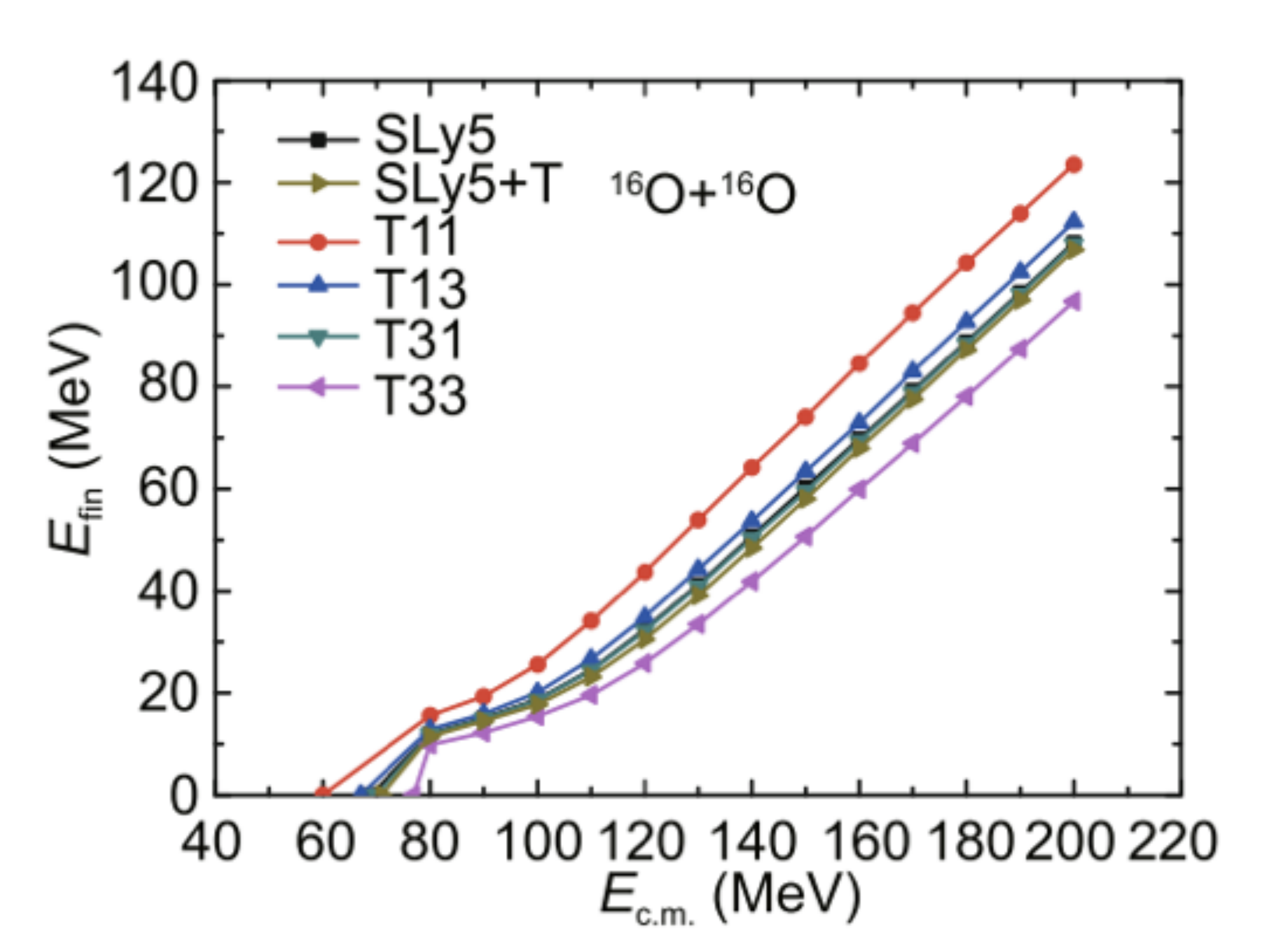

- Dai GaoFeng, Guo Lu, Zhao EnGuang & Zhou ShanGui, Science China: Phys., Mech., Astro. 57, 1618 (2014)
- Similar study but only including modification to spin-orbit strength when adding tensor terms

BOUNDARY CONDITIONS

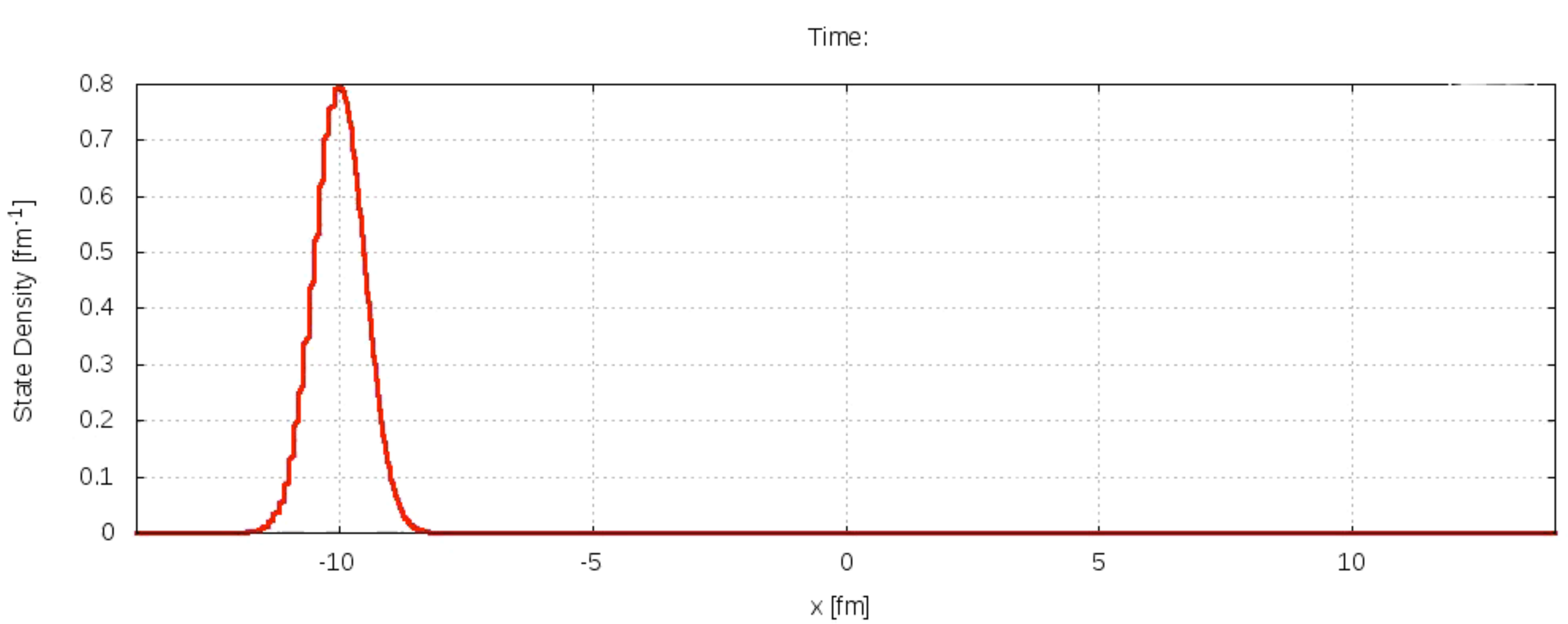

BOX SIZE DEPENDENCE

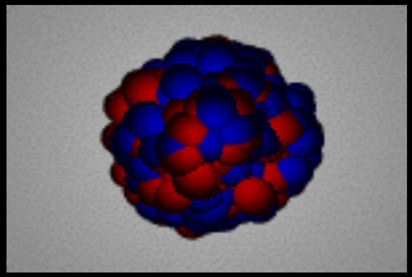

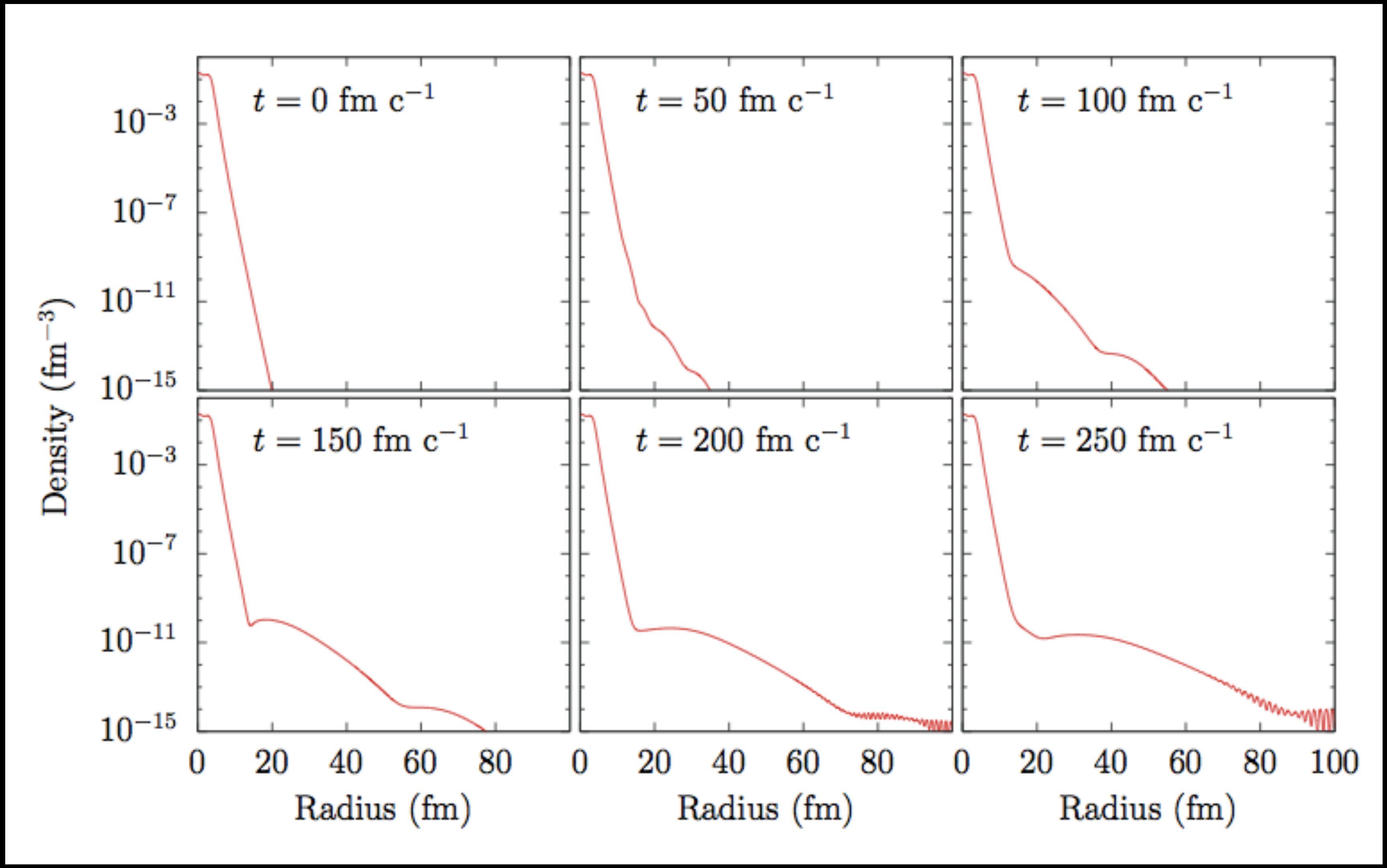

C. I. Pardi and P. D. Stevenson, Phys. Rev. **C87** 014330 (2013)

RADIUS VIBRATIONS - GMR

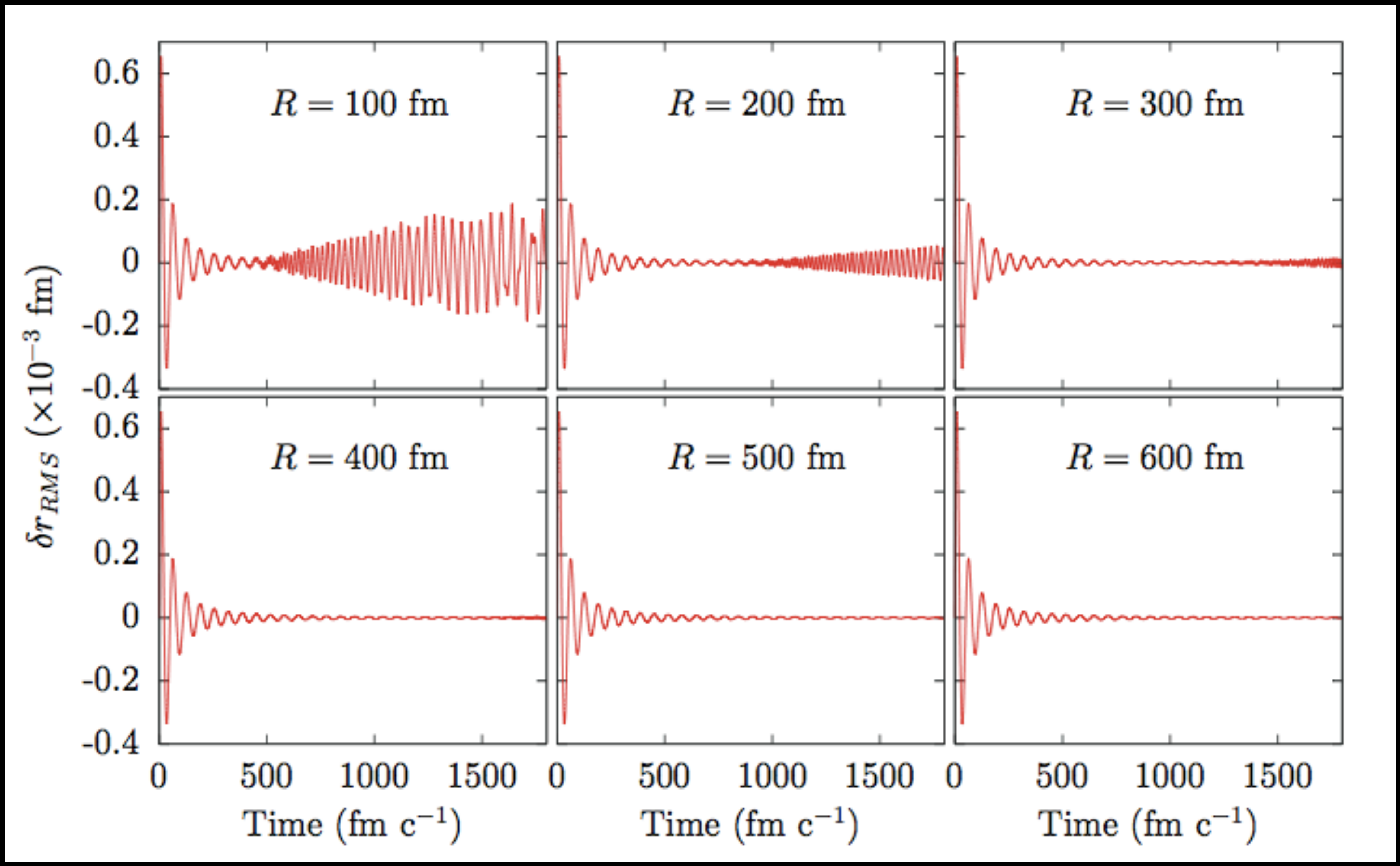

STRENGTH FUNCTIONS

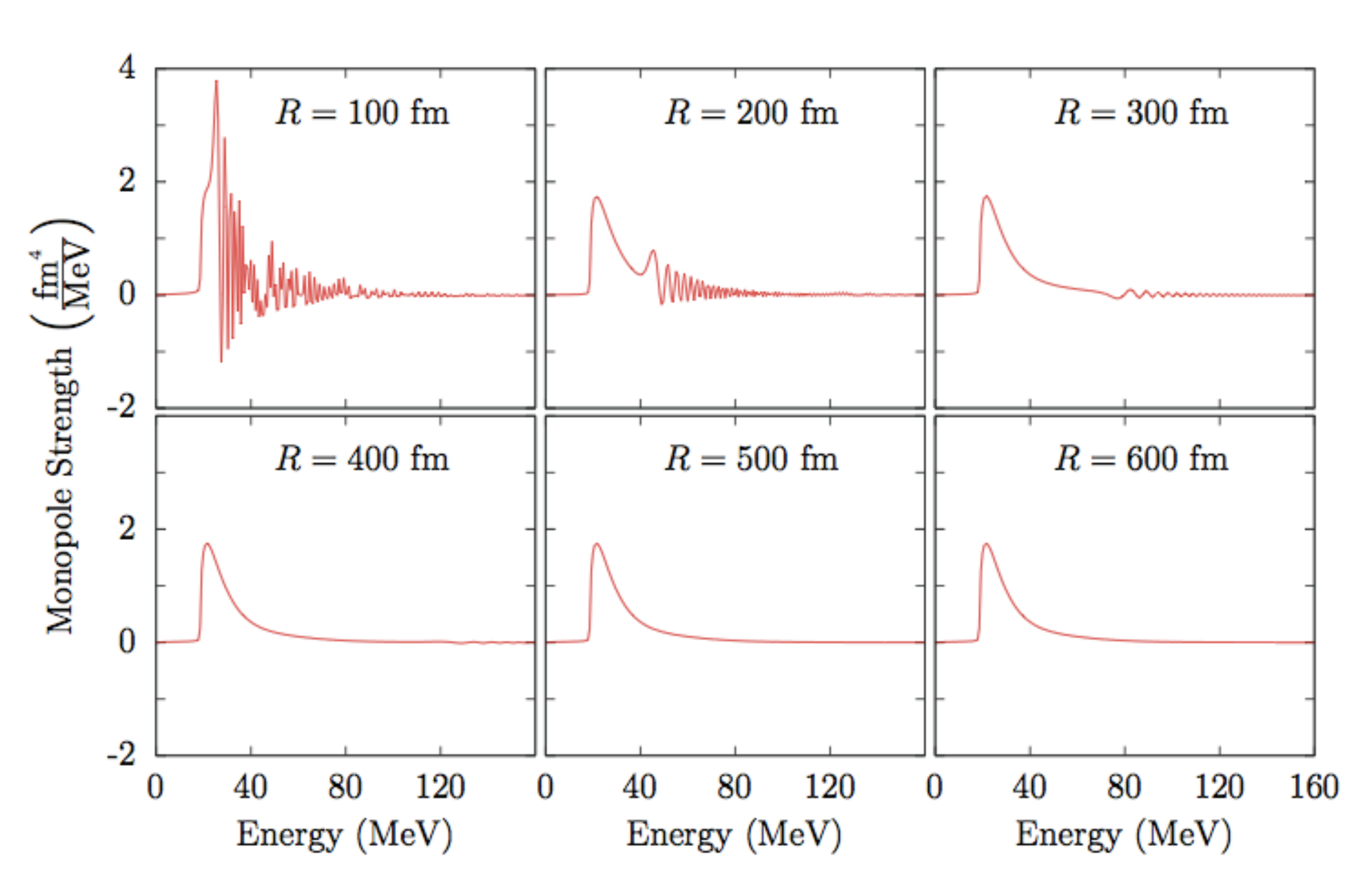

100 fm already impractical for all but spherical systems

CONTINUUM-TDHF

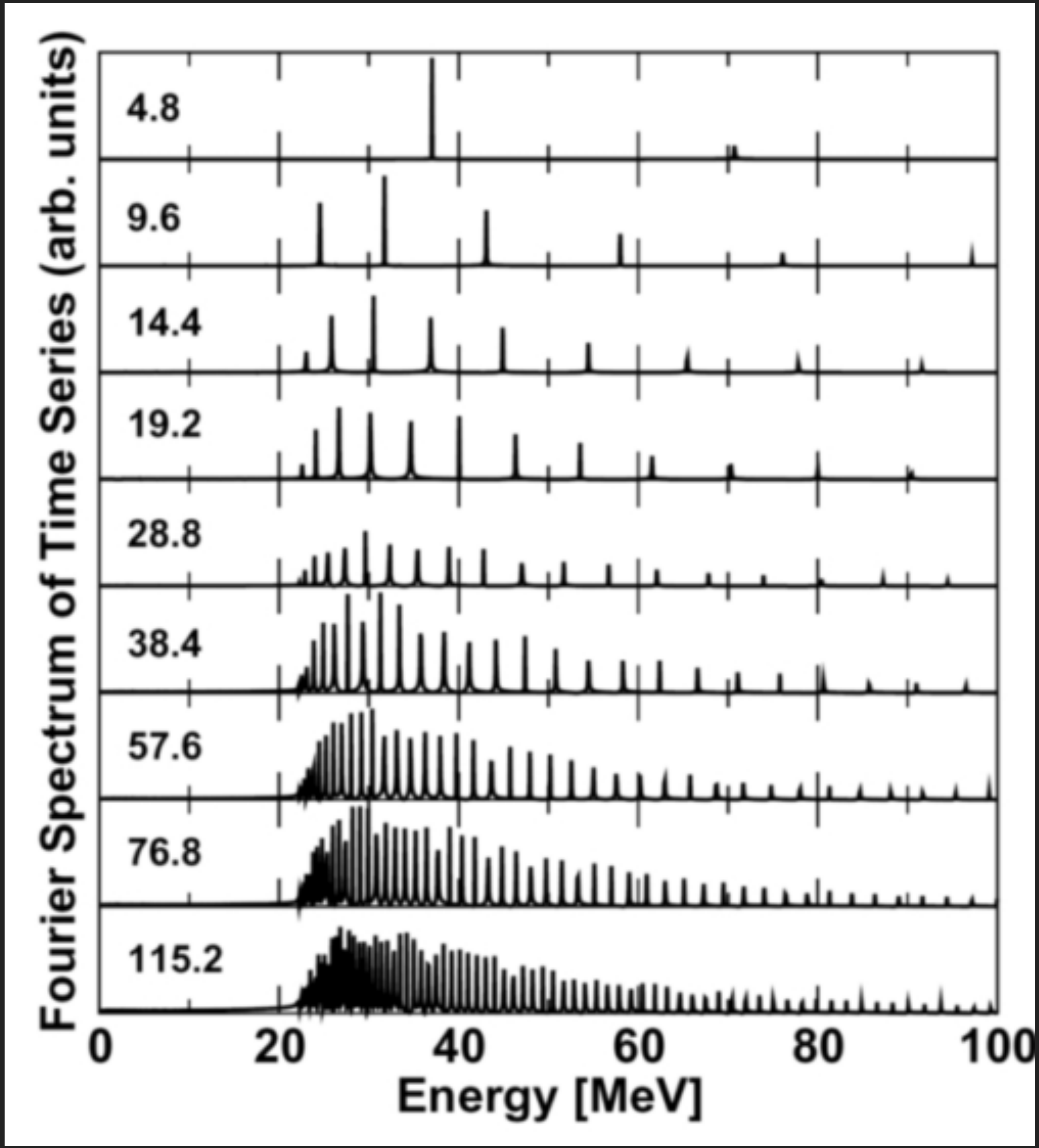

CONTINUUM TDHF

TDHF equation in dimensionless form (Q=reduced wf in spherical coords)

$$i\frac{\partial Q}{\partial t} = -\frac{1}{2}\frac{\partial^2 Q}{\partial r^2} + \left(\frac{\sigma}{r} + \frac{l(l+1)}{2r^2}\right)Q.$$

Laplace transform time coordinate

$$\frac{1}{2}\frac{\partial^2 \hat{Q}(r,s)}{\partial r^2} + \left(is - \frac{\sigma}{r} - \frac{l(l+1)}{2r^2}\right)\hat{Q}(r,s) = 0.$$

Substitute z=br√s with b=-2i√2i:

$$\frac{\partial^2 \hat{Q}(r,s)}{\partial z^2} + \left(-\frac{1}{4} + \frac{\kappa(s)}{z} - \frac{\frac{1}{4} - \mu^2}{z^2}\right)\hat{Q}(r,s) = 0$$

This is a standard tabulated form, with Whittaker function sol^{n}s

Full details in Pardi & Stevenson, PRC87, 014330 (2013)

CONTINUUM-TDHF CONT.

$$W_{\kappa,\mu}(z) \sim z^{\kappa} e^{-\frac{1}{2}z} {}_2F_0\left(\frac{1}{2}+\mu-\kappa, \frac{1}{2}-\mu-\kappa, -\frac{1}{z}\right),$$

Division of the above by its derivative and rearranging produces

$$\hat{Q}(r,s) = \frac{1}{b\sqrt{s}}\left(\frac{W_{\kappa,\mu}(br\sqrt{s})}{\frac{\partial W_{\kappa,\mu}(br\sqrt{s})}{\partial r}}\right)\frac{\partial \hat{Q}(r,s)}{\partial r}.$$

Now apply the convolution theorem and evaluate the result at r=R (the end of our box):

$$Q(R\, t) = \int_0^t G_{\kappa,\mu}(R,\tau)\frac{\partial Q(R,t-\tau)}{\partial r}\, d\tau,$$

Recall, Q is the reduced wavefunction. Note that for each each time, we have to integrate at the boundary from the beginning of time.

In the above, the kernel is the inverse Laplace transform of

$$\hat{G}_{\kappa,\mu}(R,s) = \frac{1}{b\sqrt{s}}\left(\frac{W_{\kappa,\mu}(br\sqrt{s})}{\frac{\partial W_{\kappa,\mu}(br\sqrt{s})}{\partial r}}\right)\Bigg|_{r=R}.$$

Inverse transform not totally straightforward

Full details in Pardi & Stevenson, PRC87, 014330 (2013)

INVERSE LAPLACE TRANSFORM

For neutron kernels, we have κ=0, which gives a special case of the Whittaker functions

$$W_{0,\mu}(-2ix) = \sqrt{\frac{1}{2}\pi x}\,\exp\left(\frac{1}{4}i\pi(2\mu+1)\right)H_\mu^{(1)}(x)$$

$$H_\mu^{(1)}(x) = \sqrt{\frac{2x}{\pi}}h^{(1)}_{\mu-\frac{1}{2}}(x)$$

H are Hankel functions of the first kind, and h are spherical Hankel functions. They are finite series for integer μ-1/2

These can be manipulated into a rational form (right), which can be expressed analytically in partial fractions (below)

$$\hat{G}(R,s) = \frac{-i\sum_{v=0}^{l}\left[\frac{(l+\frac{1}{2},v)}{(l+\frac{3}{2},0)(-2iR)^v}\right]k^{l-v}}{k^{l+1}+\sum_{v=0}^{l}\left[\frac{(l+\frac{3}{2},v+1)-2(l+1)(l+\frac{1}{2},v)}{(l+\frac{3}{2},0)(-2iR)^{v+1}}k^{l-v}\right]}.$$

$$\left(l+\frac{1}{2},j\right) = \frac{(l+j)!}{j!\,(l-j)!}$$

$$\begin{aligned}\hat{G}_l(R,s) &= \sum_{j=1}^{l+1}\frac{\alpha_j}{k-k_j}\\ &= \sum_{j=1}^{l+1}\frac{\frac{\alpha_j}{\sqrt{2i}}}{\sqrt{s}-\frac{k_j}{\sqrt{2i}}}.\end{aligned}$$

Full details in Pardi & Stevenson, PRC87, 014330 (2013)

INVERSE LAPLACE TRANSFORMATION

Use linearity of Laplace transformation & tabulated form of partial fraction expansion:

$$\mathcal{L}^{-1}\left\{\frac{1}{\sqrt{s}+a}\right\} = \frac{1}{\sqrt{\pi t}} - a\mathrm{w}(ia\sqrt{t}),$$

Where w is the Fadeeva function $w(z)=\exp(-z^2)\mathrm{erfc}(-iz)$

Some further simplification yields

$$G_l(R,\tau) = \frac{-i}{\sqrt{2\pi i \tau}} - \frac{i}{2}\sum_{j=1}^{l+1} \alpha_j k_j \mathrm{w}\left(z_j\right).$$

This is then discretised in space and time coordinates, and is the basis for what is evaluated at the boundary.

What about protons? What about Coulomb?

Life *does* get quite a bit harder.

(We think that) there is no convenient analytic rearrangement of the kernel into partial fractions or similar form with tabulated inverse Laplace transform

Instead, we assume a rational, finite, polynomial form and fit to the Whittaker functions with a non-linear least squares method. The finite polynomial is again expanded in partial fractions

Extension of the continuum time-dependent Hartree-Fock method to proton states

Phys. Rev. E **89**, 033312 (2014)

C. I. Pardi, P. D. Stevenson, and K. Xu

CONTINUUM TDHF

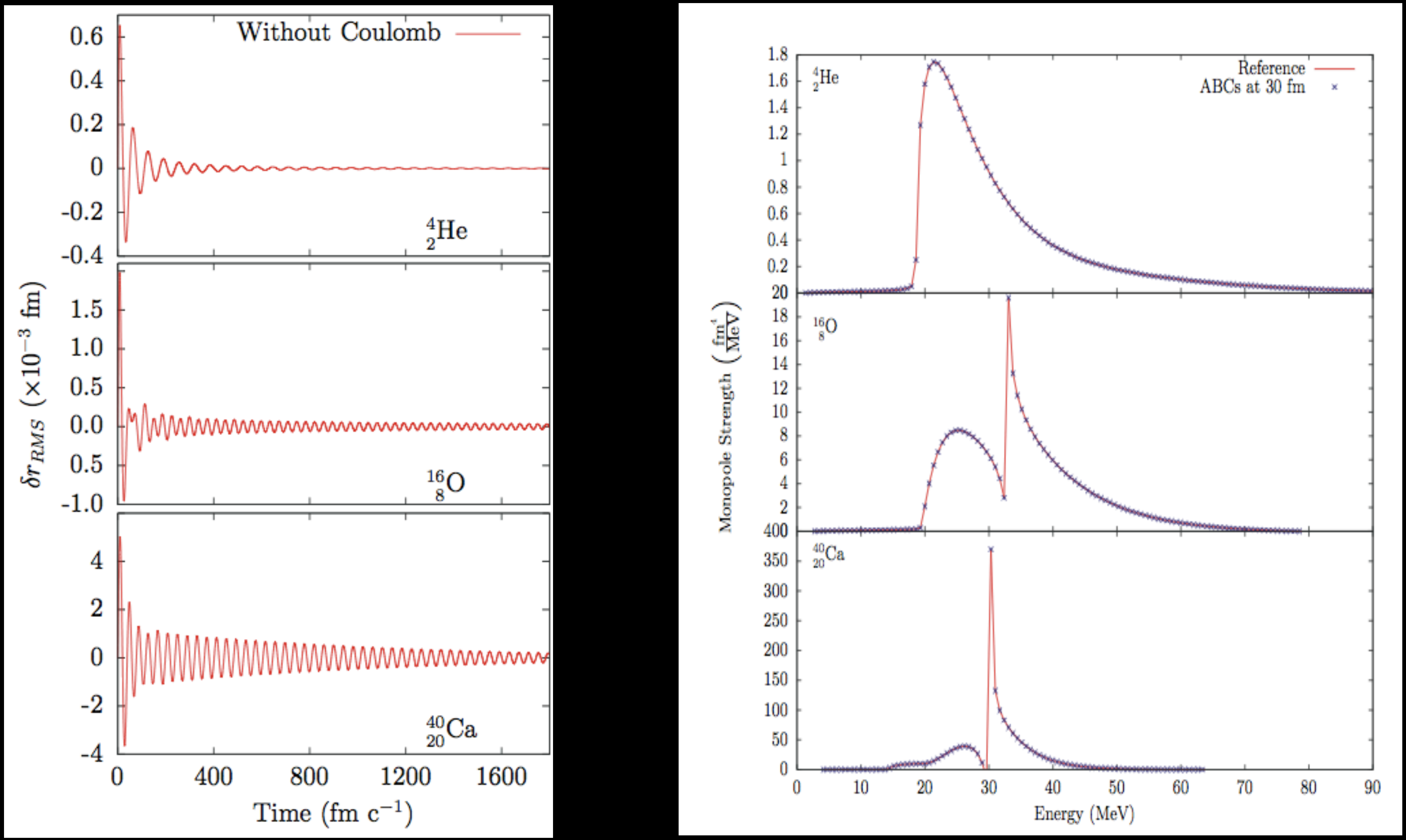

Some very long-lived components = fine structure in the strength

Continuum-TDHF with Coulomb in C. I. Pardi, P. D. Stevenson and K. Xu, arXiv: 1306.4500, accepted for publication in PRE

FISSION IN TDHF

- Large amplitude collective motion
- can in principle think of performing induced fission, starting from an excited state
- TDHF cannot deal with spontaneous fission since it is deterministic in terms of trajectories of collective variables

QUADRUPOLE LANDSCAPE IN ^{240}PU

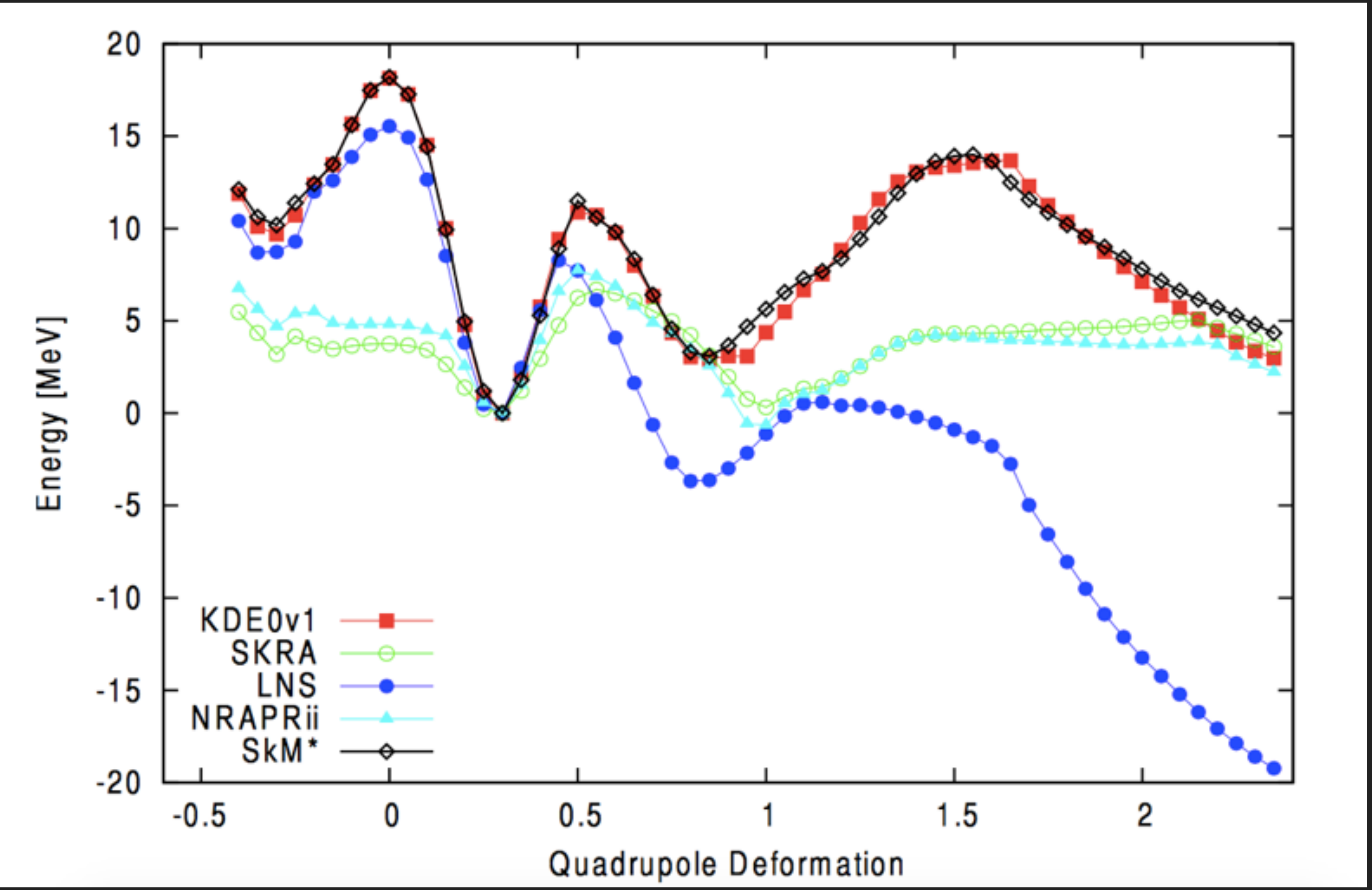

FISSION IN ^{240}PU

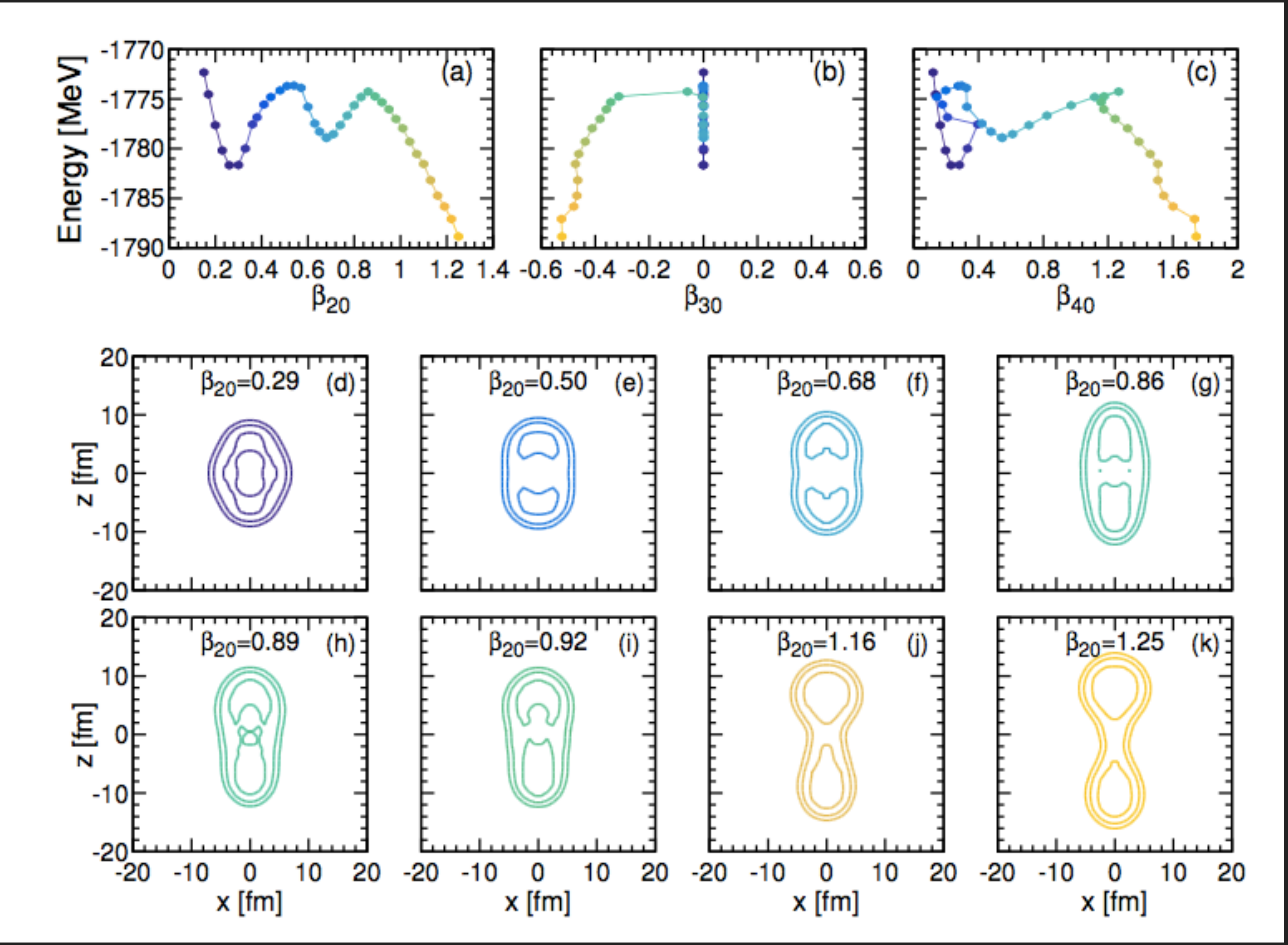

BOOST-INDUCED FISSION

Starting from fission isomer, we give the nucleus a quadrupole boost

a large amount of energy needs to be pumped in to the quadrupole mode so that enough of it goes into the fission pathway

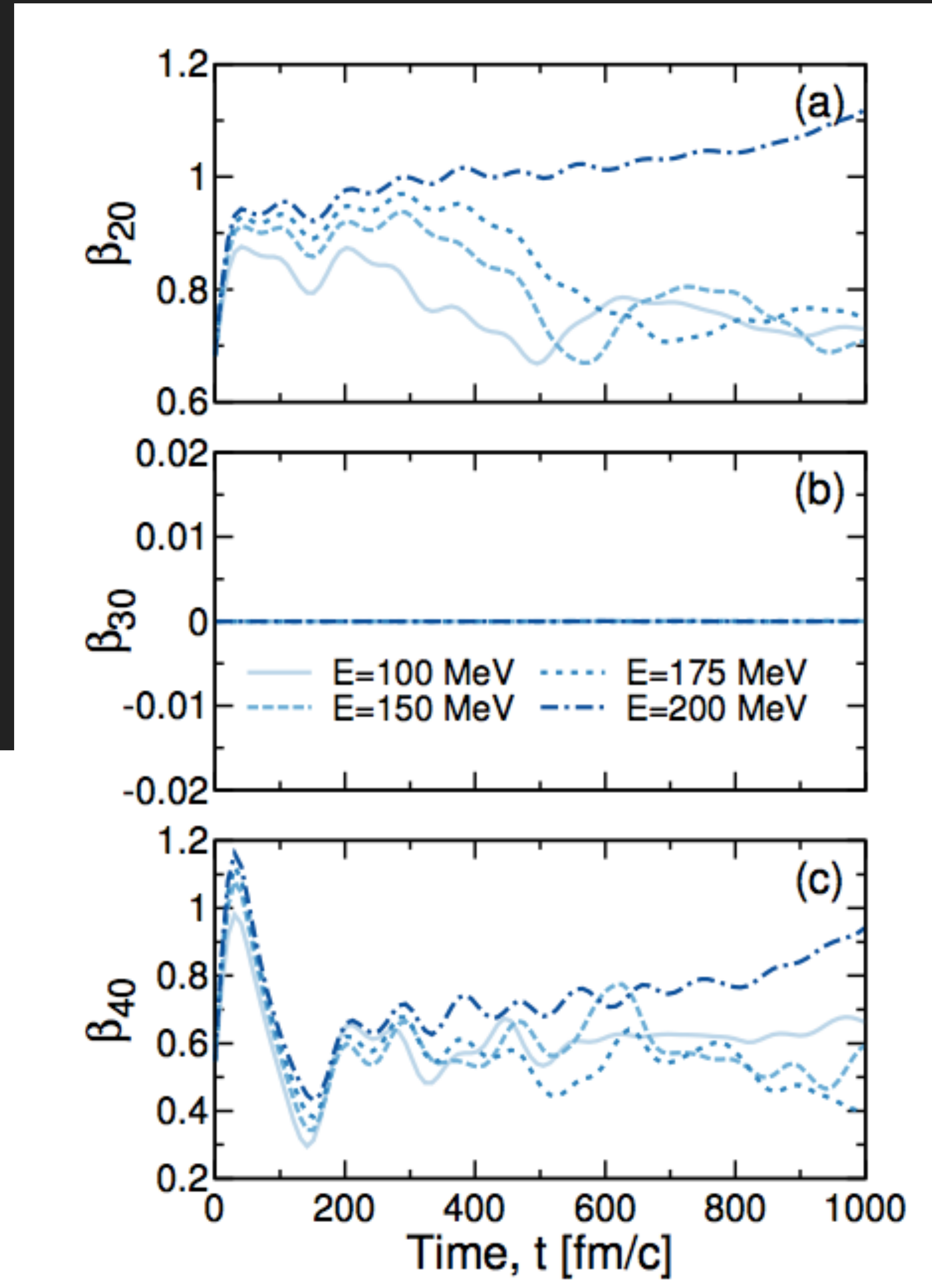

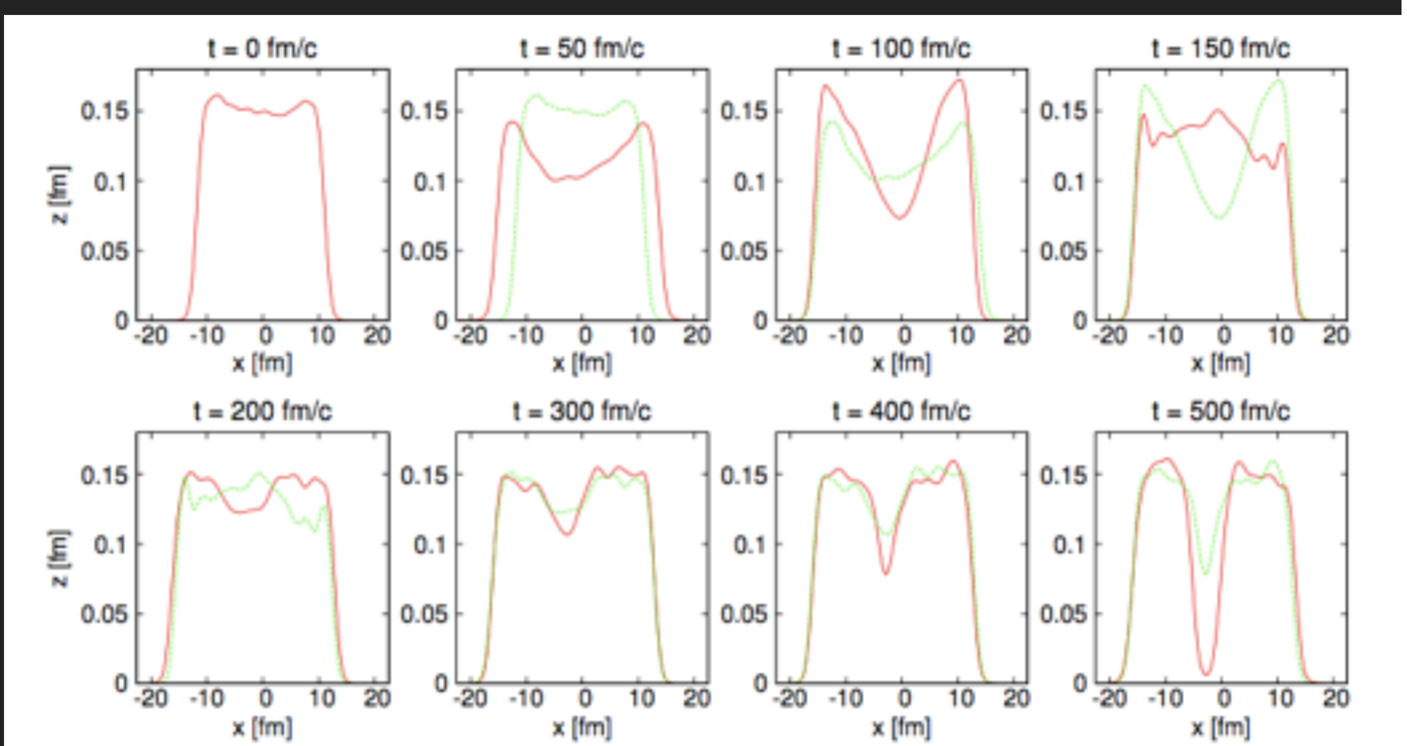

FISSION

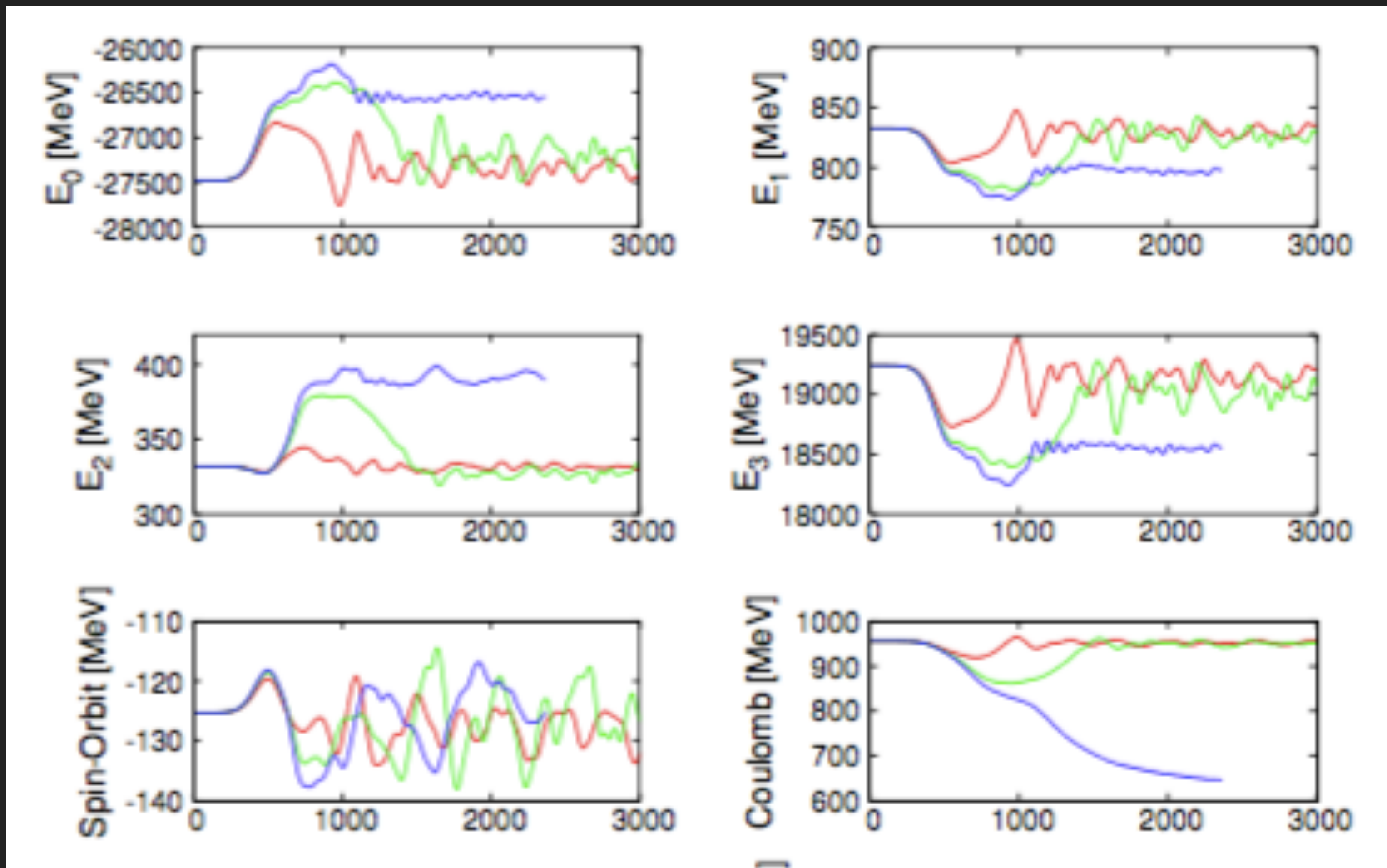

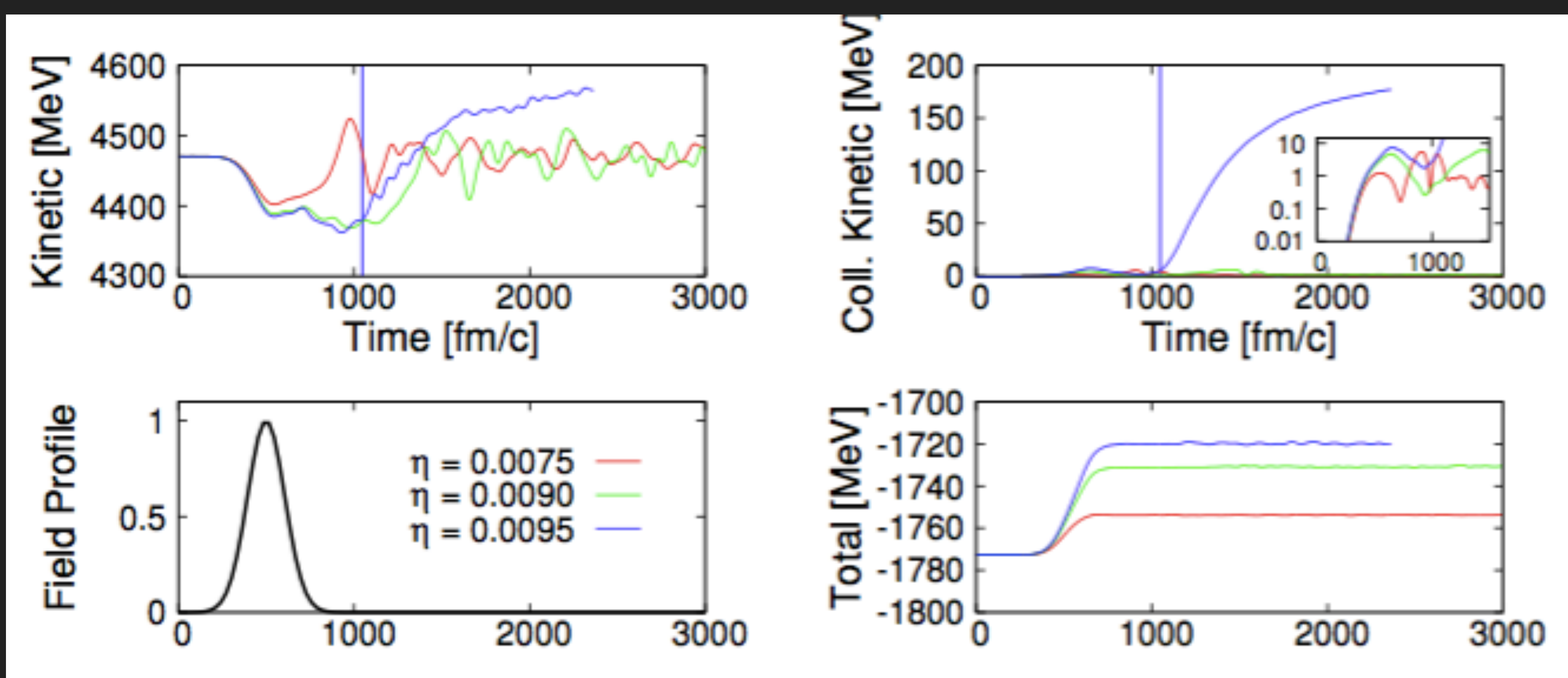

Apply time-dependent boost

quadrupole mode gets induced more gently, with low-frequency modes getting excited with higher amplitude that high-frequency modes

fission occurs with tens, not hundreds of MeV

P. M. Goddard, PhD thesis, Surrey (2014)

DEFORMATION-INDUCED FISSION

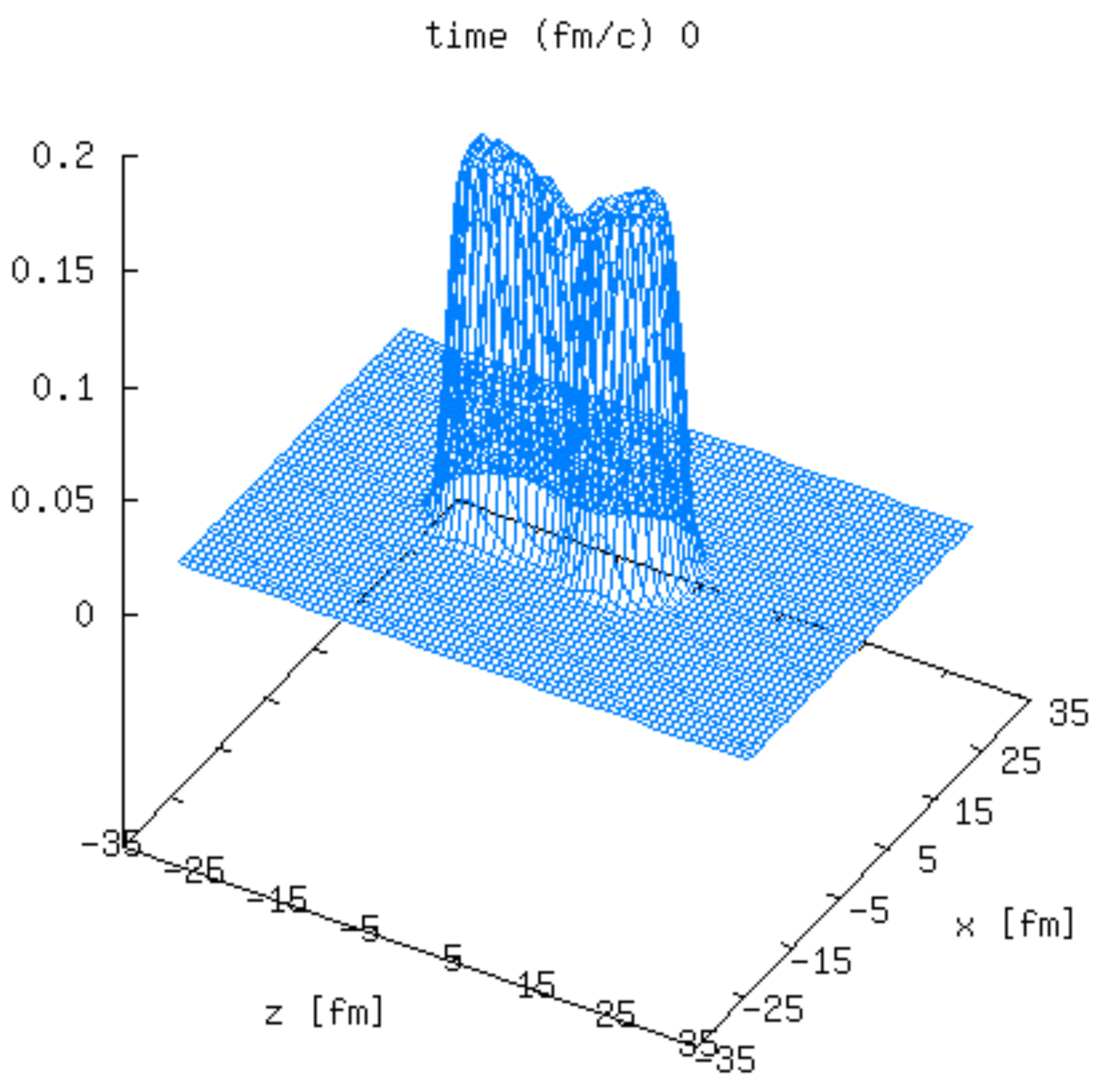

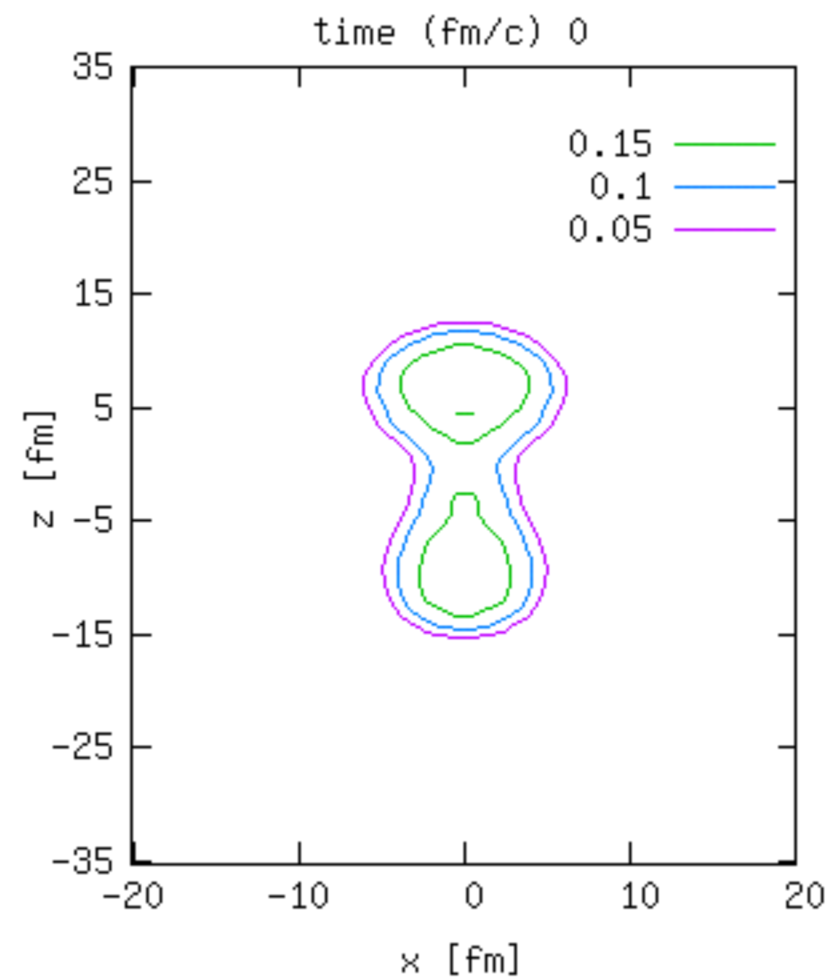

SAMPLE OF DIFFERENT STARTING POINTS

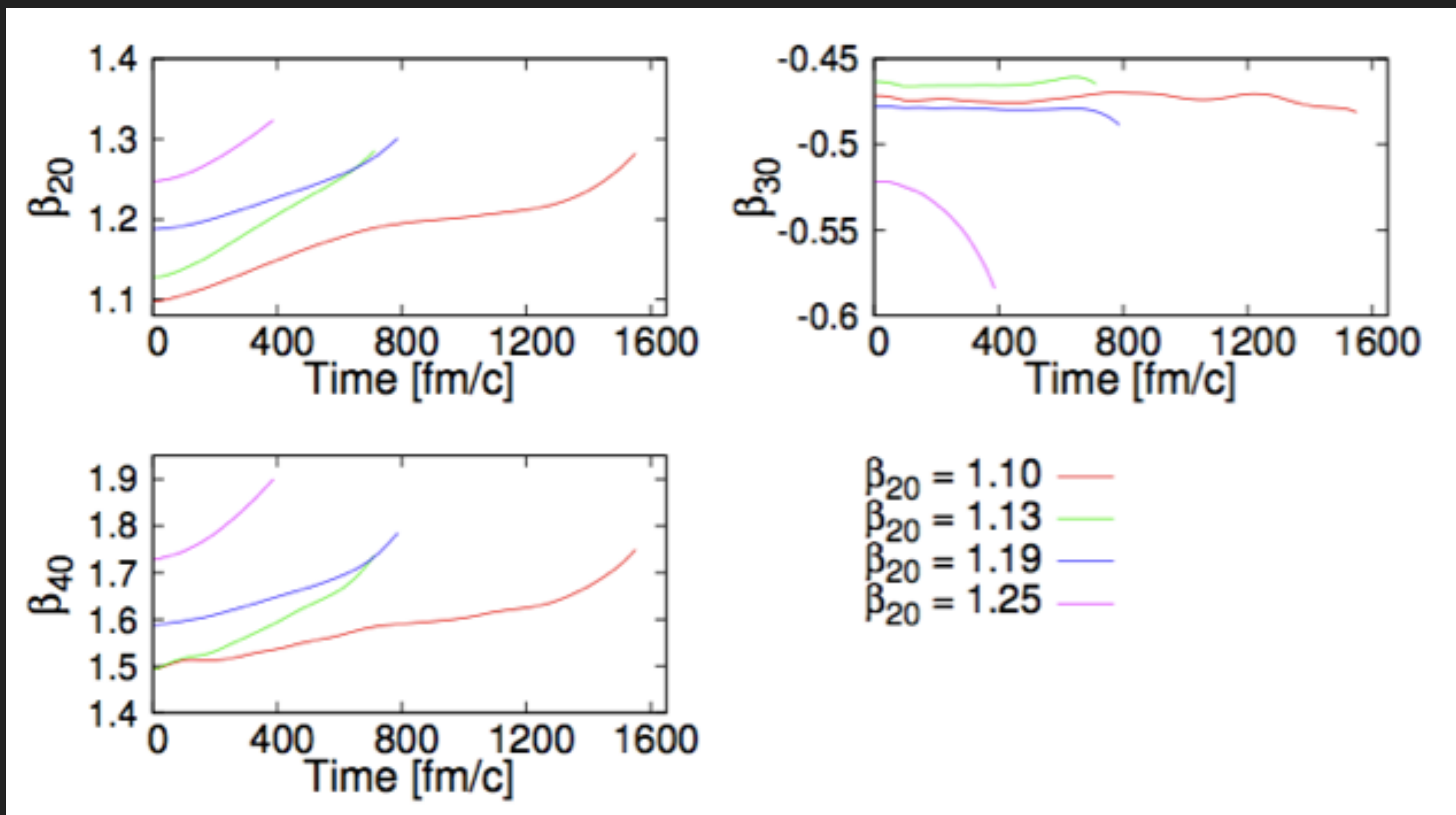

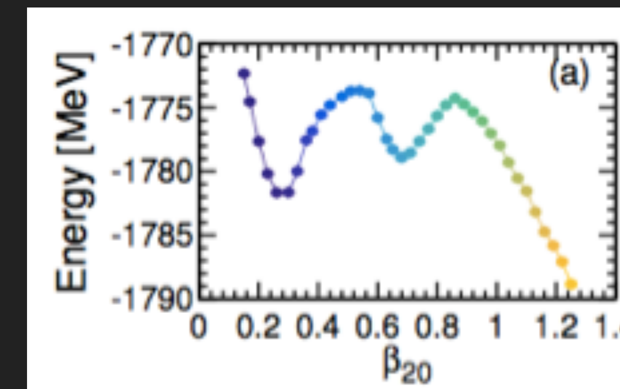

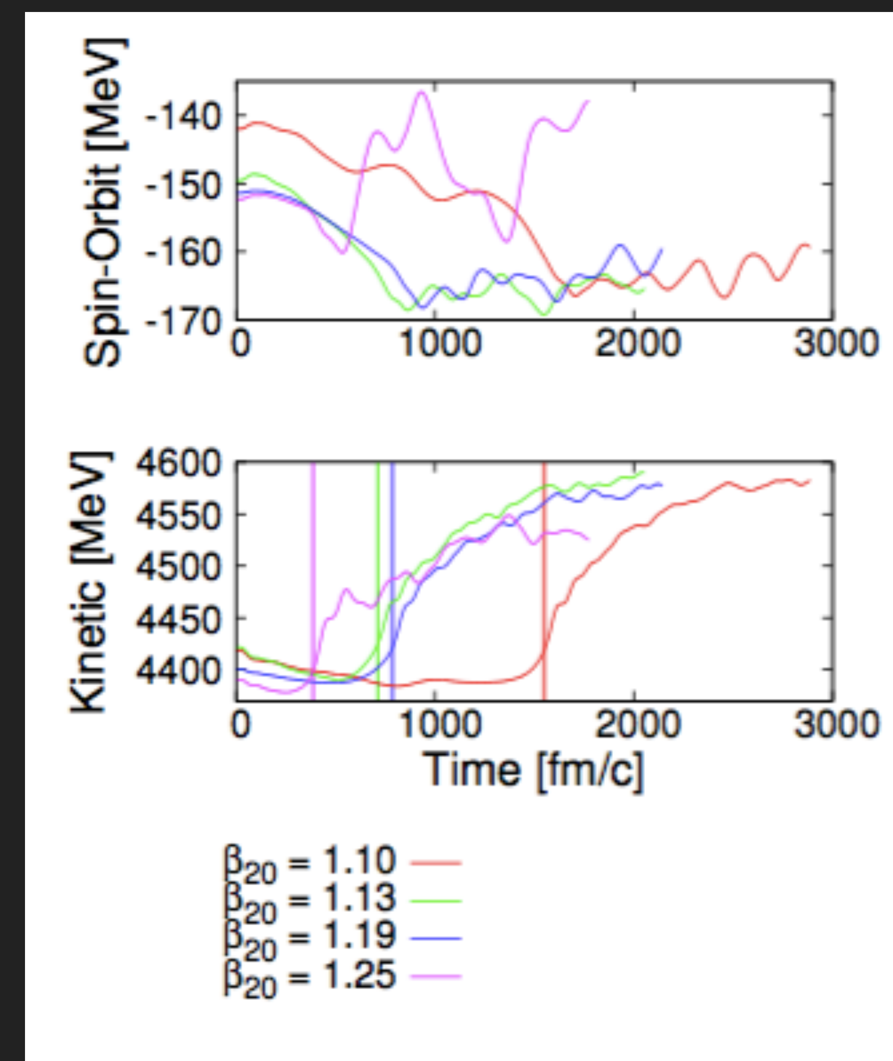

non-adiabatic paths – leads to a kind of fragment distribution

FRAGMENT DISTRIBUTION

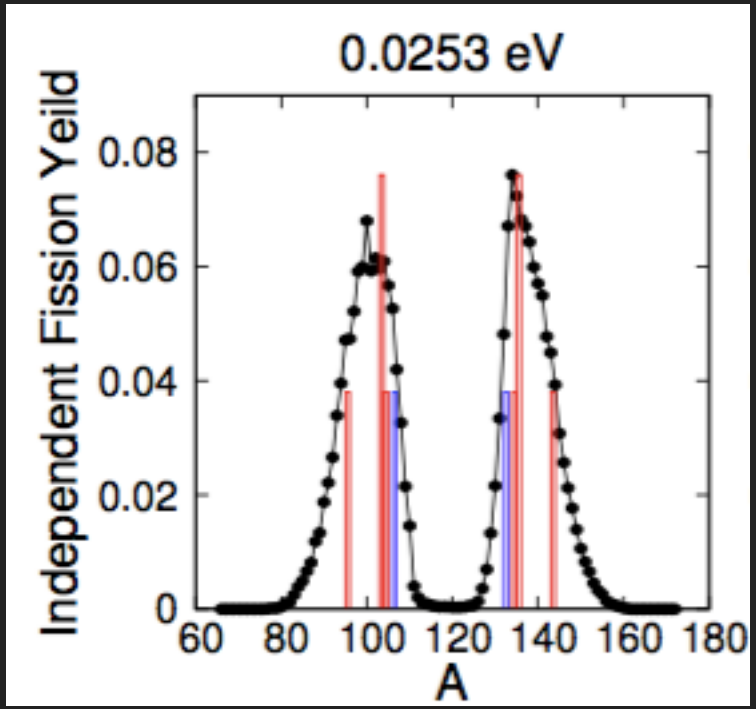

Static β_{20}	Heavy Frag.	E^* [MeV]	E_{gs} [MeV]	ΔE [MeV]	Light Frag.	E^* [MeV]	E_{gs} [MeV]	ΔE [MeV]
1.10	${}^{136}_{53}I$	-1029.22	-1118.31	89.09	${}^{104}_{41}Nb$	-747.86	-854.54	106.68
1.13	${}^{135}_{52}Te$	-1023.81	-1110.24	86.43	${}^{105}_{42}Mo$	-757.38	-865.71	108.33
1.19	${}^{136}_{53}I$	-1034.23	-1118.31	84.04	${}^{104}_{41}Nb$	-749.41	-854.54	105.13
1.25	${}^{144}_{55}Cs$	-1090.17	-1162.47	72.30	${}^{96}_{38}Sr$	-697.78	-796.94	99.16

POWER SPECTRUM OF FRAGMENTS

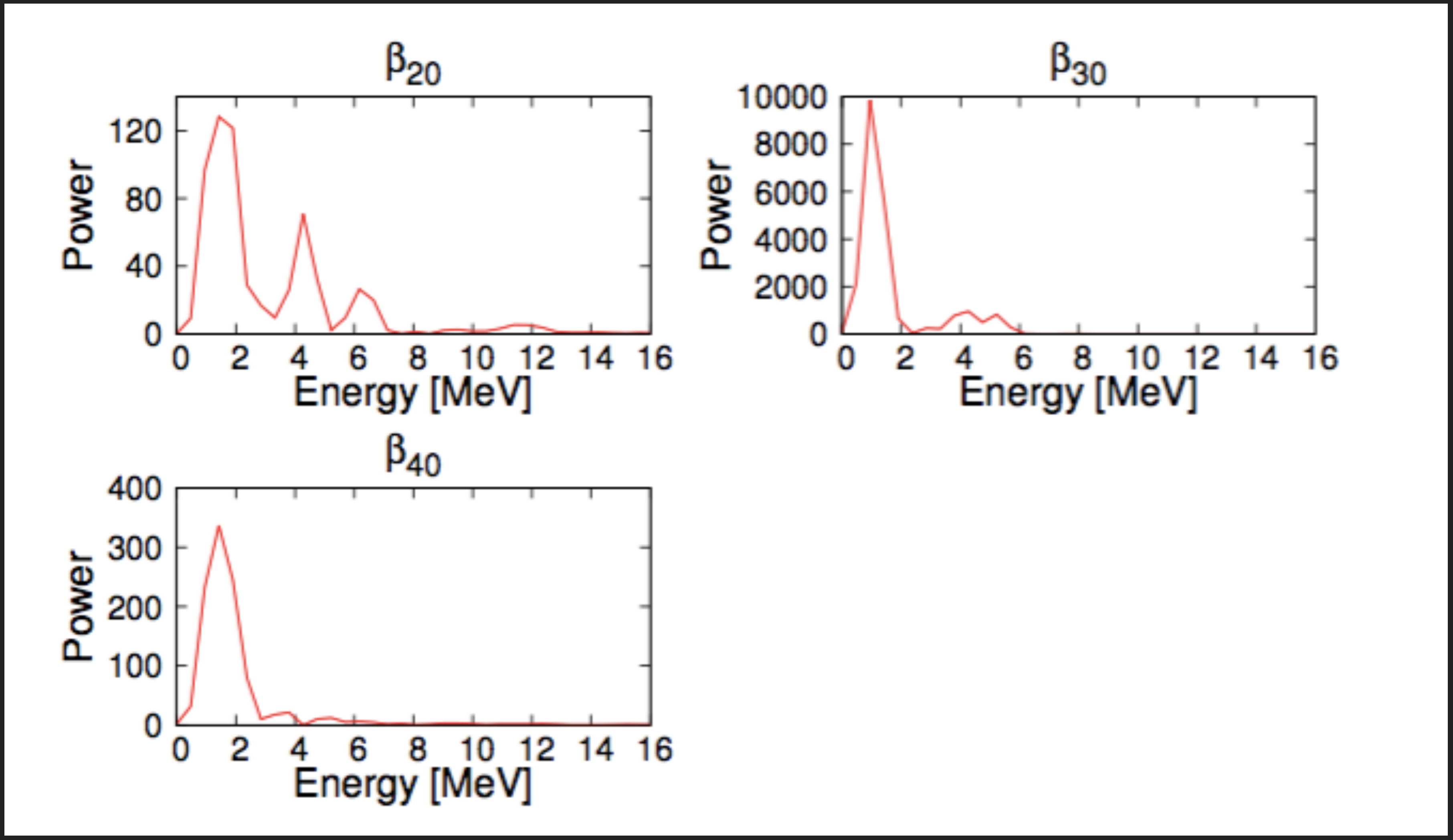

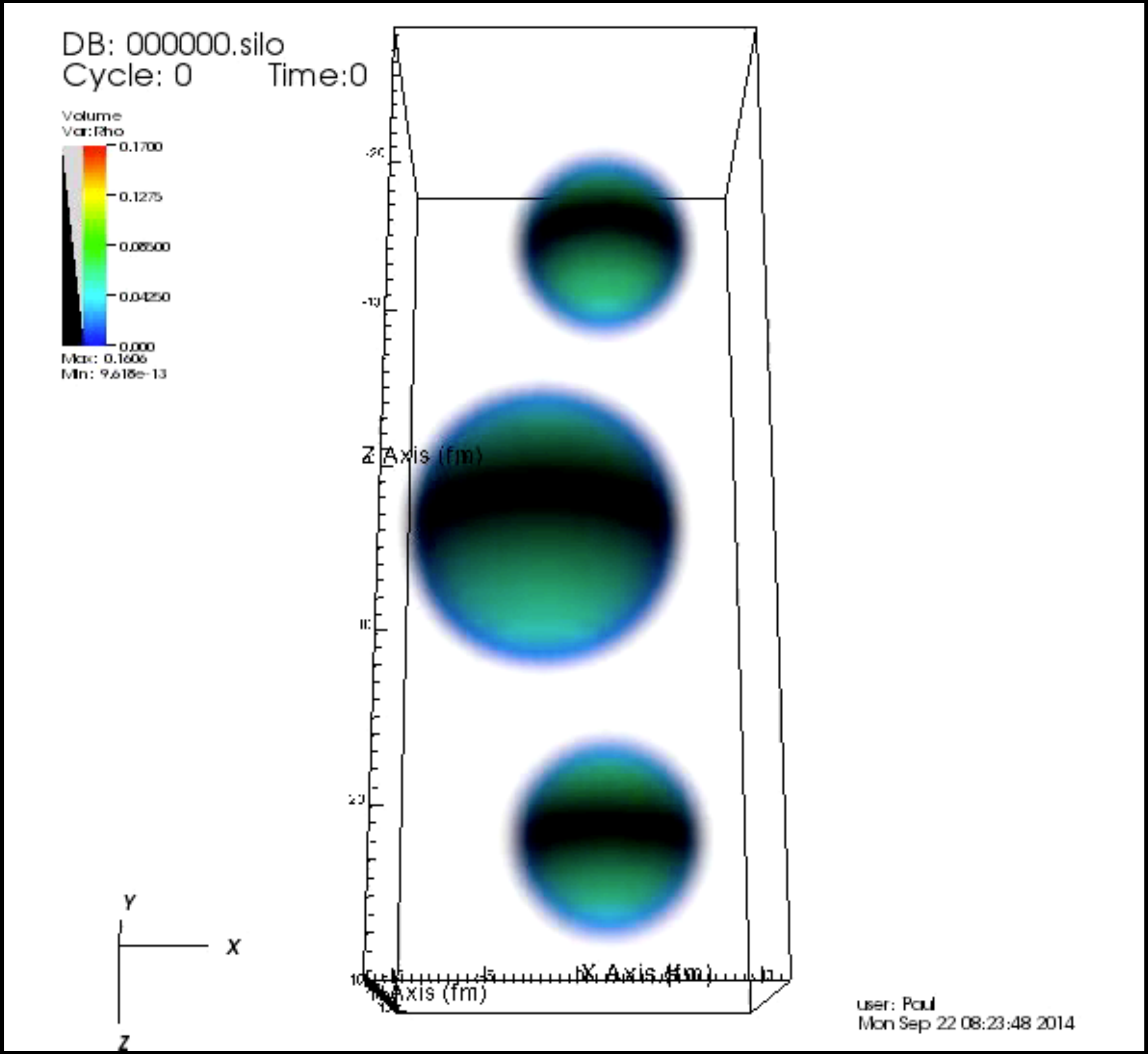
DB: 000000.silo
Cycle: 0 Time:0
Volume
Var:Rho
0.1700
0.1275
0.08500
0.04250
0.000
Max: 0.1606
Min: 9.618e-13
Z Axis (fm)
X Axis (fm)
Y Axis (fm)
Y
X
Z
user: Paul
Mon Sep 22 08:23:48 2014

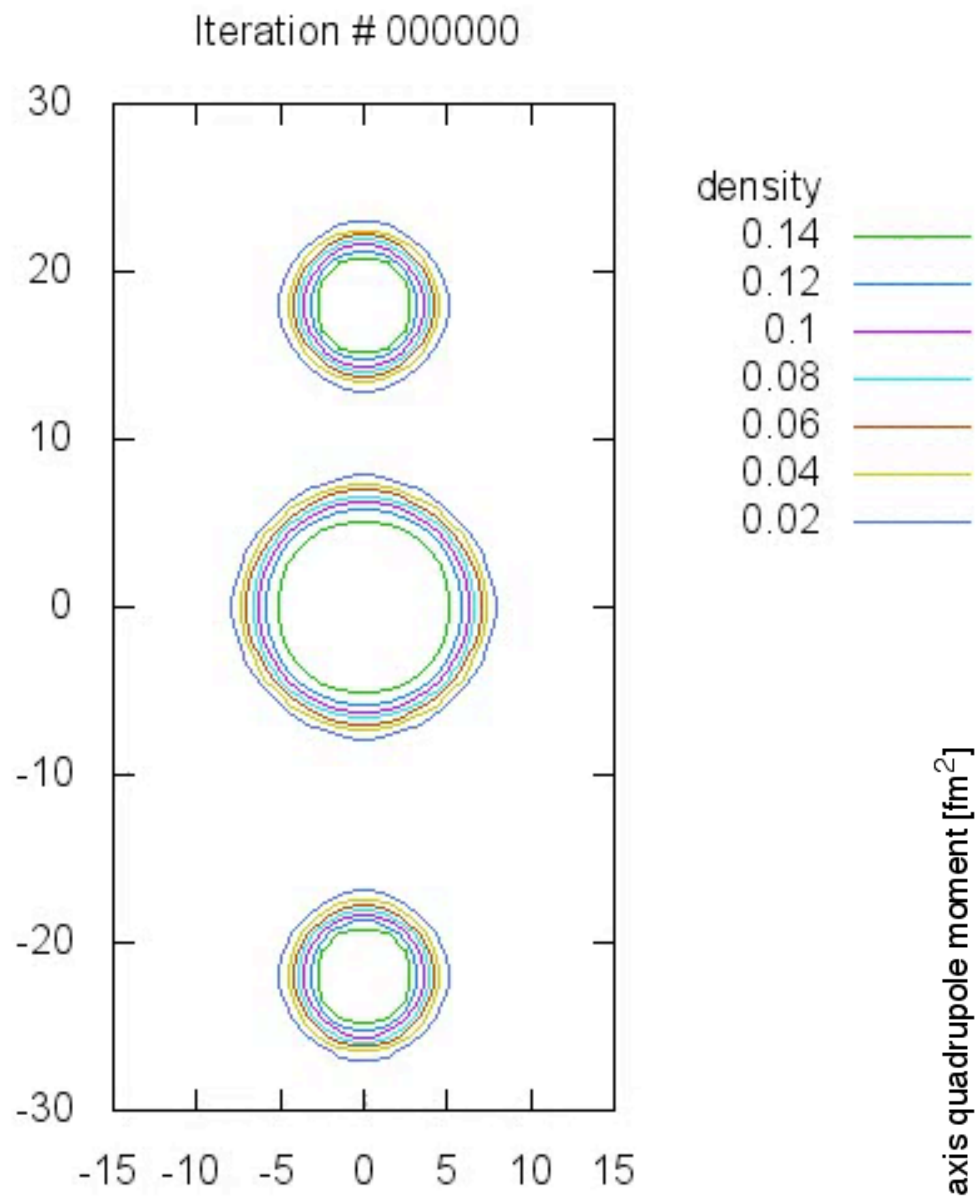
Iteration # 000000
density
0.14
0.12
0.1
0.08
0.06
0.04
0.02
30
20
10
0
-10
-20
-30
-15
-10
-5
0
5
10
15

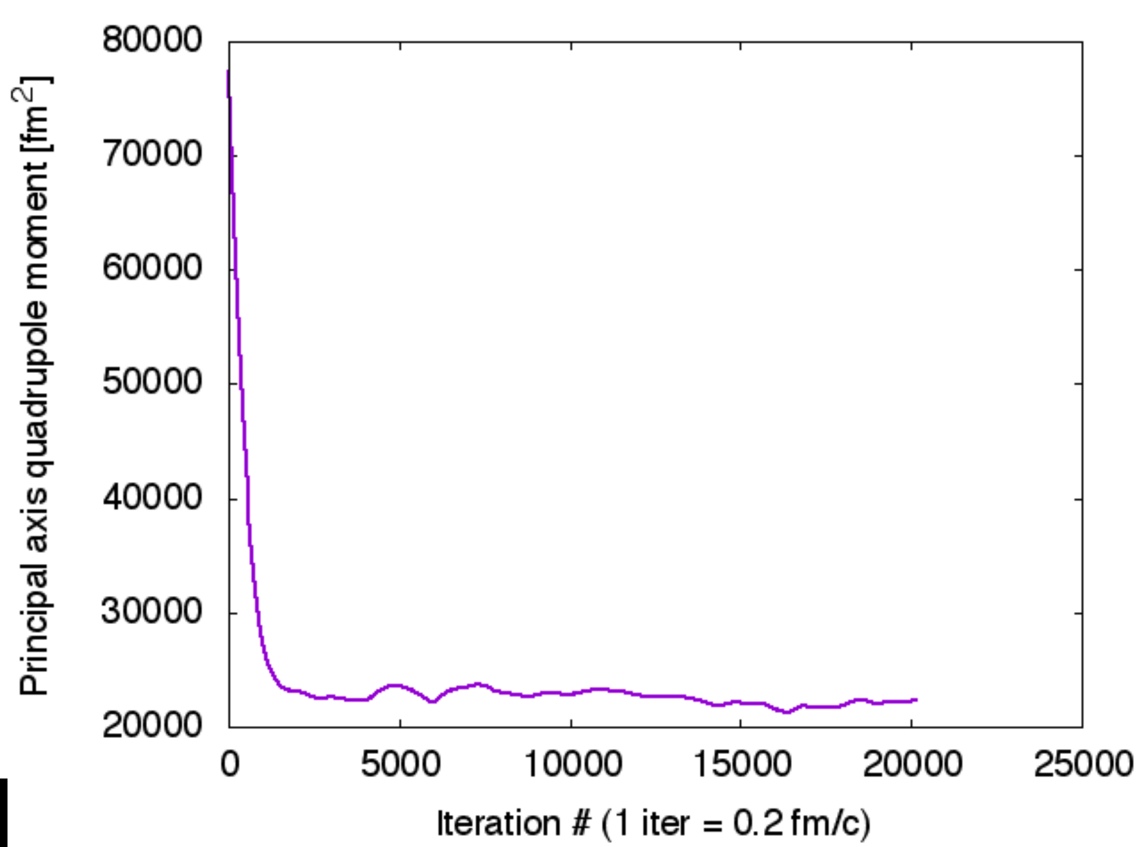
Principal axis quadrupole moment [fm^2]
80000
70000
60000
50000
40000
30000
20000
0
5000
10000
15000
20000
25000
Iteration # (1 iter = 0.2 fm/c)

CONSTRAINING K'

- ISGQR dominated by single peak
- extract energy from one cycle (automatically a continuum calculation)
- correlate energy with K'
- K'=400±30 MeV

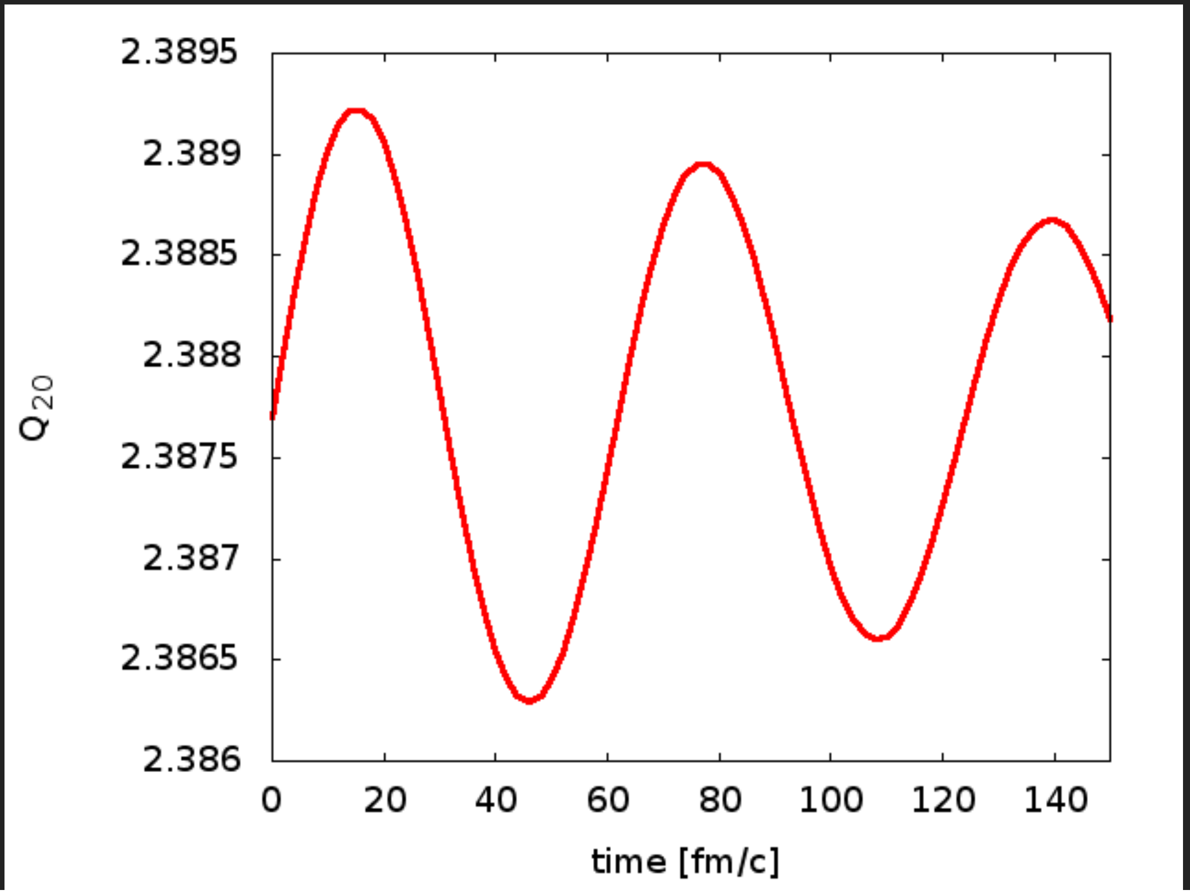

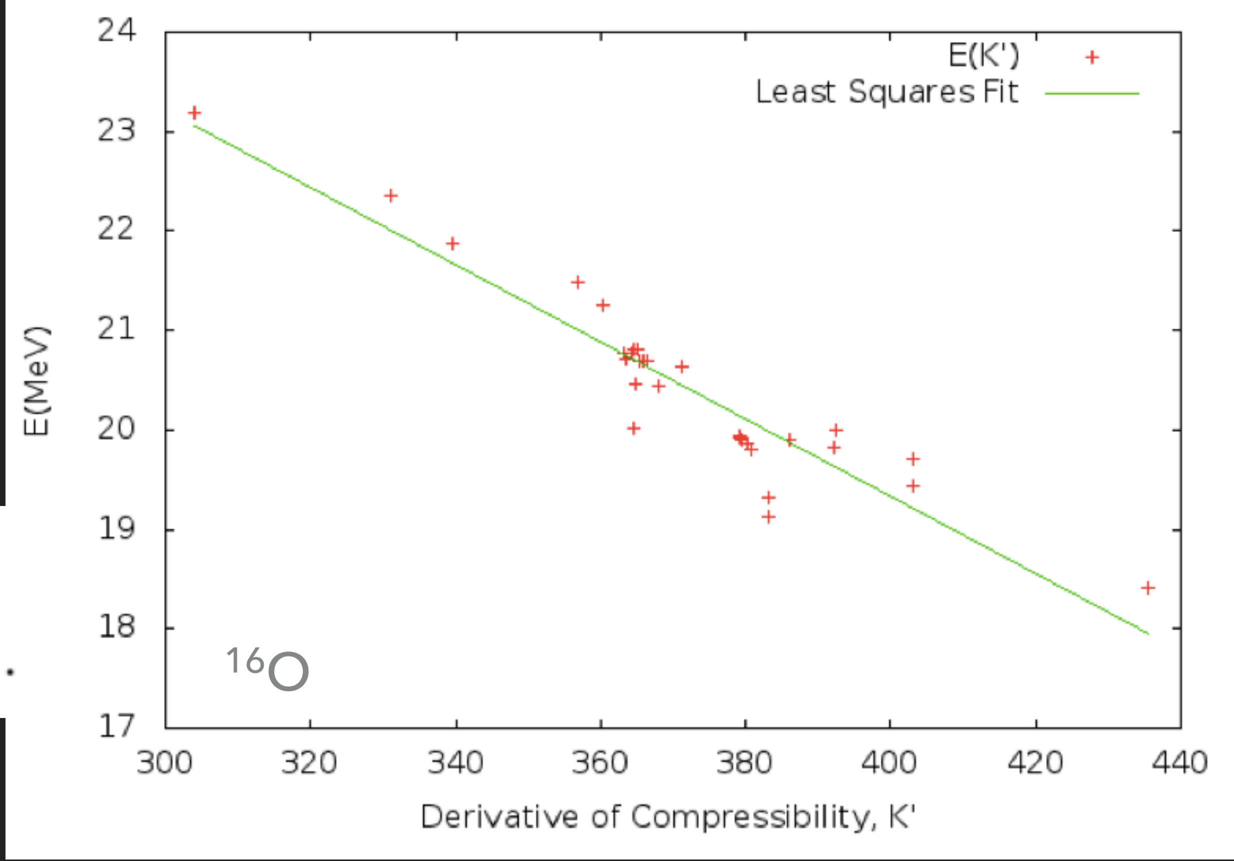

$$e^{\infty}(\rho,\eta) = a_v + (K_v/18)\epsilon^2 - (K'/162)\epsilon^3 + \ldots$$
$$+\eta^2\{J + (L/3)\epsilon + (K_{\mathrm{sym}}/18)\epsilon^2 - (K'_{\mathrm{sym}}/162)\epsilon^3 + \ldots\} + \ldots$$

$\epsilon \equiv (\rho - \rho_0)/\rho_0$ $\eta \equiv (\rho_n - \rho_p)/\rho$

- TDHF applied to large & small amplitude motion
- Effect of choice of Skyrme parameterisation and what time-odd terms are used can be significant
- computationally expensive to systematically study too many interactions or include in fits – especially for some processes (like fission)